

Two-Tier Precoding for FDD Multi-cell Massive MIMO Time-Varying Interference Networks

Junting Chen, *Student Member, IEEE* and Vincent K. N. Lau, *Fellow, IEEE*

Abstract—Massive MIMO is a promising technology in future wireless communication networks. However, it raises a lot of implementation challenges, for example, the huge pilot symbols and feedback overhead, requirement of real-time global CSI, large number of RF chains needed and high computational complexity. We consider a two-tier precoding strategy for multi-cell massive MIMO interference networks, with an outer precoder for inter-cell/inter-cluster interference cancellation, and an inner precoder for intra-cell multiplexing. In particular, to combat with the computational complexity issue for the outer precoding, we propose a low complexity online iterative algorithm to track the outer precoder under time-varying channels. We follow an optimization technique and formulate the problem on the Grassmann manifold. We develop a low complexity iterative algorithm, which converges to the global optimal solution under static channels. In time-varying channels, we propose a compensation technique to offset the variation of the time-varying optimal solution. We show with our theoretical result that, under some mild conditions, perfect tracking of the target outer precoder using the proposed algorithm is possible. Numerical results demonstrate that the two-tier precoding with the proposed iterative compensation algorithm can achieve a good performance with a significant complexity reduction compared with the conventional two-tier precoding techniques in the literature.

Index Terms—Massive MIMO, Two-tier Precoding, Tracking Algorithm, Optimization, Grassmann Manifold

I. INTRODUCTION

Massive MIMO is a promising technology to meet the future capacity demand in wireless cellular networks. Equipped with a large number of antennas, the system has a sufficient number of degrees of freedom (DoF) to exploit the *spatial multiplexing gains* for intra-cell users and to mitigate the *inter-cell interference*. However, the corresponding beamforming (precoder) designs for such multiuser MIMO (MU-MIMO) interference networks are challenging even in traditional MIMO systems with a small number of antennas. In [1], the inter-cell interference is mitigated by using coherently coordinated transmission (CCT) from multiple base stations (BSs) to each user, using commonly shared global channel state information (CSI). In [2], the beamformers are jointly optimized among BSs, where the uplink-downlink duality is used to obtain the global CSI in a time-division duplex (TDD) system. Using alternative optimization techniques, WMMSE algorithm is proposed in [3] with the objective to maximize the weighted sum rate for multi-cell systems. Moreover, interference alignment (IA)

approaches were used in [4], [5] for downlink interference cellular networks.

We consider the beamforming design for frequency-division duplex (FDD)¹ massive MIMO systems with a large number of antennas N_t . Unlike conventional multi-cell MU-MIMO networks, where the schemes in [1]–[5] may be easily implemented, FDD massive MIMO systems induce a lot of practical issues: (i) *huge pilot symbols and feedback overheads*, (ii) *large number of RF chains*, (iii) *real-time global CSI sharing*, and (iv) *huge computational complexity* for precoders at the BSs. For instance, the required number of independent pilot symbols for transmit side CSI (CSIT) estimation at the mobile scales as $\mathcal{O}(N_t)$, and so as the CSIT feedback overheads. In addition, as N_t scales up, the number of RF chains also scales up, which induces a high fabrication cost and power consumption. Although the dynamic antenna switching techniques [6], [7] may reduce the required number of RF chains, those solutions did not fully utilize the benefits of the extra antennas. Moreover, there is signaling latency over the backhauls and it is highly difficult to acquire global real-time CSIT for precoding. Finally, the computational complexity for the precoding algorithms scales quickly with N_t , and low complexity precoding algorithms are needed for massive MIMO systems.

In this paper, we address all the above difficulties by considering a *two-tier precoding with subspace alignments*. This is motivated by the clustering behavior of the user terminals. As illustrated in Fig. 1, the users in the same cluster may share the same scattering environment, and hence, they may have similar spatial channel correlations. Whereas, users from a different cluster may have different spatial channel correlations. Therefore, we can decompose the MIMO precoder at the BS into an *outer precoder* and an *inner precoder*. The outer precoder is used to mitigate *inter-cell* and *inter-cluster* interference based on the statistical channel spatial covariance. Since the spatial correlations are slowly varying, the outer precoder can be computed on a slower timescale. On the other hand, the inner precoder is used for spatial multiplexing of intra-cluster users on the dimension-reduced subspace spanned by the outer precoder. As a result, the inner precoders are adaptive to the local real-time CSIT at the BS and can be computed in a faster timescale. Using the proposed *two-tier precoding structure*, we shall illustrate in Section III-B that the aforementioned technical issues (i)–(iii) associated with large N_t can be substantially alleviated.

This paper was accepted in IEEE Journal on Selected Areas in Communications, special issue on 5G wireless communication systems.

The authors are with the Department of Electronic and Computer Engineering (ECE), The Hong Kong University of Science and Technology (HKUST), Hong Kong (e-mail: {ejtchen, eeknlau}@ust.hk).

¹FDD is still a major duplexing technique in the near future, especially for macro-coverage applications.

In [8], [9], a zero-forcing based two-tier precoding has been proposed for single cell massive MIMO systems. The outer precoders are computed using a block diagonalization (BD) algorithm. However, it requires a high complexity for computing the outer precoder, and the tracking issues for the outer precoder under time-varying channels were not addressed. In fact, the computational complexity is a serious concern in massive MIMO systems as the number of antennas scales to very large. For example, in the BD algorithm proposed in [8], [9], we need to apply a series of matrix manipulations including SVD to a number of $N_t \times N_t$ channel covariance matrices each time we update the outer precoder, and the associated complexity is $\mathcal{O}(N_t^3)$. In addition, deriving a low complexity iterative algorithm for the BD solution in [8], [9] is far from trivial. To address the complexity issue, we consider online tracking solutions to exploit the temporal correlation of the channel matrices. There is a body of literature for iterative subspace tracking algorithms, for example, gradient-based algorithms [10]–[13], power iteration based algorithms [14] and the algorithms based on Krylov subspace approximations [15], [16]. Moreover, the author in [17] proposed an iterative subspace tracking precoder design for MIMO cellular networks. However, these algorithms have not fully exploited the channel temporal correlations to enhance the tracking. In this paper, we propose a compensated subspace tracking algorithm for the online computation of the outer precoder. The algorithm is derived by solving an optimization problem formulated on the Grassmann manifold, and its tracking capability is enhanced by introducing a compensation term that estimates and offsets the motion of the target signal subspace. Using a control theoretical approach, we also characterize the tracking performance of the online outer precoding algorithm in time-varying massive MIMO systems. We show that, under mild technical conditions, perfect tracking (with zero convergence error) of the target outer precoder using the proposed compensation algorithm is possible, despite the channel covariance matrix being time-varying. In general, we demonstrate with numerical results that the proposed two-tier precoding algorithm has a good system performance with low signaling overhead and low complexity of $\mathcal{O}(N_t^2)$.

The rest of the paper is organized as follows. Section II introduces the massive MIMO channel model and the signal model. Section III illustrates the two-tier precoding techniques. Section IV derives the iterative algorithm for tracking the outer precoder, where the associated convergence analysis is given in Section V. Numerical results are given in Section VI and Section VII gives the concluding remarks.

Notations: We use lower case bold font to denote vectors and upper case bold font for matrices. \mathbf{I}_N denotes the $N \times N$ identity matrix. For matrices $\mathbf{A} \in \mathbb{C}^{N \times p}$ and $\mathbf{B} \in \mathbb{C}^{N \times q}$, $[\mathbf{A} \ \mathbf{B}]$ denotes a $N \times (p+q)$ concatenated matrix, whose first p columns are given by \mathbf{A} and the last q columns are given by \mathbf{B} .

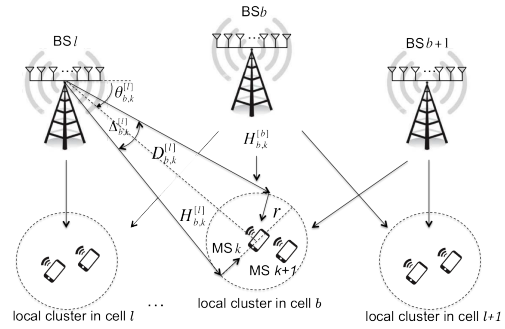


Figure 1. A multiuser MIMO cellular network. The channel is modeled by a one-ring local scattering model, where the MS is surrounded by a scattering ring with radius r .

II. SYSTEM MODEL

A. Massive MIMO Channel Model with Local Spatial Scattering

We consider a cellular network with G BSs, and the b -th ($1 \leq b \leq G$) BS serves K_b MSs. The MSs are clustered together, and without loss of generality, we assume each BS serves one cluster of MSs². Each BS has N_t antennas and each user has N_r antennas. The downlink channel from the l -th BS to the k -th MS in the b -th cell is given by $\mathbf{H}_{b,k}^{[l]} \in \mathbb{C}^{N_r \times N_t}$. The receive signal at the MS k in cell b is given by

$$\mathbf{y}_{b,k} = \mathbf{H}_{b,k}^{[b]} \mathbf{x}^{[b]} + \sum_{l=1, l \neq b}^G \mathbf{H}_{b,k}^{[l]} \mathbf{x}^{[l]} + \mathbf{n}_{b,k}$$

where $\mathbf{x}^{[l]} \in \mathbb{C}^{d_l}$ is the symbol transmitted at the BS l , d_l is the number of data streams transmitted by BS l , and $\mathbf{n}_{b,k} \sim \mathcal{CN}(0, \mathbf{I}_{N_r})$ is the additive complex Gaussian noise.

In the massive MIMO system, where the BS has a large number of antennas ($N_t \gg 1$) and is placed on the top of a building, there is usually not enough local scattering surrounding the BS. Correspondingly, it has also been shown by channel measurements that most of the signal energy is localized over the azimuth direction [18]. Therefore, we consider the one-ring local scattering model [19], [20] to characterize the massive MIMO channel. As illustrated in Fig. 1, the local scattering surrounding the MS is modeled by a ring with radius r ; whereas, the transmit signal from the BS shapes a narrow *angular spread* (AS) denoted as $\Delta_{b,k}^{[l]} \approx 2 \tan^{-1}(r/D_{b,k}^{[l]})$, where $D_{b,k}^{[l]}$ is the distance between BS l and MS k in cell b . Let $\theta_{b,k}^{[l]}$ be the angle of departure (AoD) of a path from BS l to MS k in cell b . We use the von-Mises model to characterize the *power azimuth spectrum* (PAS) w.r.t. $\theta_{b,k}^{[l]}$ [19], [21] as follows:

$$\mathbb{P}_{\theta, (b,k)}^{[l]}(\theta_{b,k}^{[l]}) = \frac{\exp \left[\kappa_{b,k}^{[l]} \cos(\theta_{b,k}^{[l]} - \bar{\theta}_{b,k}^{[l]}) \right]}{2\pi J_0(\kappa_{b,k}^{[l]})}, \quad (1)$$

where $\bar{\theta}_{b,k}^{[l]}$ is the mean angle of the AoD, J_0 is the zeroth order modified Bessel function and $\kappa_{b,k}^{[l]} = (2\Delta_{b,k}^{[l]})^{-2}$

²Note that the extension to the case of multiple clusters is very straight forward. Hence we only focus on the single cluster case to simplify the notation.

characterizes the AS at BS l in the direction of MS k in cell b . Denote $\mathbf{T}_{b,k}^{[l]}$ as the corresponding transmit spatial correlation matrix at BS l . The (p, q) -th entry of the matrix $\mathbf{T}_{b,k}^{[l]}$, which describes the spatial correlations between the p -th and q -th antenna elements at BS l [22], is defined as:

$$\left[\mathbf{T}_{b,k}^{[l]}\right]_{(p,q)} = \int_{-\pi}^{\pi} e^{j[\phi_p^{[l]}(\theta) - \phi_q^{[l]}(\theta)]} \mathbb{P}_{\theta, (b,k)}^{[l]}(\theta) d\theta \quad (2)$$

where $\phi_p^{[l]}(\theta) - \phi_q^{[l]}(\theta)$ accounts for the phase difference between the p -th and q -th antenna elements over the azimuth direction θ at BS l .

We assume that MSs within the same cluster have the same channel statistical parameters $\bar{\theta}_{b,k}^{[l]}$ and $\kappa_{b,k}^{[l]}$, i.e., $\bar{\theta}_{b,k}^{[l]} = \bar{\theta}_{b,j}^{[l]}$ and $\kappa_{b,k}^{[l]} = \kappa_{b,j}^{[l]}$, $\forall j$. As a result, the transmit correlation matrices satisfy $\mathbf{T}_{b,k}^{[l]} = \mathbf{T}_{b,j}^{[l]} \triangleq \mathbf{T}_b^{[l]}$ for all MS in the scattering cluster of cell b . We adopt the following two-timescale, clustered, and spatial correlated massive MIMO channel model.

Assumption 1: (Two-timescale, Clustered and Spatial Correlated Channel Model) The time-varying massive MIMO channel $\mathbf{H}_{b,k}^{[l]}(j)$ on each subframe j is given by

$$\mathbf{H}_{b,k}^{[l]}(j) = \mathbf{H}_k^\omega(j) \mathbf{T}_b^{[l]}(j)^{1/2} \quad (3)$$

where $\mathbf{H}_k^\omega(j)$ and $\mathbf{T}_b^{[l]}(j)$ are changing in different timescales:

- **Small Timescale:** $\mathbf{H}_k^\omega(j)$ are identical and independently distributed (i.i.d.) over MSs k and is time-varying over subframes j . Each element of the matrix \mathbf{H}_k^ω follows an independent complex Gaussian distribution with zero mean and unit variance.
- **Large Timescale:** The spatial correlation matrix $\mathbf{T}_b^{[l]}(j)$ is constant within each super-frame $(n-1)T_s < j \leq nT_s$, but changes between consecutive super-frames (i.e., a block of T_s subframes).

B. Signal Model, Interference Mitigation and Challenges

Denote the precoding matrix for user k in cell b as $\mathbf{V}_k^{[b]} \in \mathbb{C}^{N_t \times d_{b,k}}$ and the associated receiver shaping matrix as $\mathbf{U}_{b,k} \in \mathbb{C}^{N_r \times d_{b,k}}$, where $d_{b,k}$ is the number of the data streams. Applying the receiver shaping matrix $\mathbf{U}_{b,k}$ to the signal $\mathbf{y}_{b,k}$ at MS k in cell b , the received signal is given by

$$\begin{aligned} \hat{\mathbf{y}}_{b,k} = & \mathbf{U}_{b,k}^\dagger \mathbf{H}_{b,k}^{[b]} \mathbf{V}_k^{[b]} \mathbf{s}_k^{[b]} + \underbrace{\mathbf{U}_{b,k}^\dagger \mathbf{H}_{b,k}^{[b]} \sum_{j=1, j \neq k}^{K_b} \mathbf{V}_j^{[b]} \mathbf{s}_j^{[b]}}_{\text{intra-cell interference}} \\ & + \underbrace{\mathbf{U}_{b,k}^\dagger \sum_{l=1, l \neq b}^G \mathbf{H}_{b,k}^{[l]} \sum_{j=1}^{K_l} \mathbf{V}_j^{[l]} \mathbf{s}_j^{[l]}}_{\text{inter-cell interference}} + \hat{\mathbf{n}}_{b,k} \end{aligned} \quad (4)$$

where $\hat{\mathbf{n}}_{b,k} = \mathbf{U}_{b,k}^\dagger \mathbf{n}_{b,k}$ is still a standard complex Gaussian noise and $\mathbf{s}_j^{[l]} \in \mathbb{C}^{d_{l,j}}$ is the data symbol intended for user j in cell l . The per BS power budget is $\sum_{j=1}^{K_b} \text{tr}(\mathbf{V}_j^{[b]} \mathbf{V}_j^{[b]\dagger}) \leq P$.

In the conventional approach, the inter-cell interference mitigation and intra-cell spatial multiplexing are achieved by a joint design of the precoders $\mathbf{V}_k^{[b]}$ and receiver shaping matrices $\mathbf{U}_{b,k}$ among all the BSs using, for example, ZF techniques [23], [24], WMMSE [3], IA [5], [25], etc. However, these approaches cannot be directly applied in FDD massive MIMO cellular systems because:

- A large number of RF chains (N_t) are required to perform RF-baseband translation as well as Analog-to-Digital (A/D) conversion. As a result, there is a huge cost in hardware design and power consumption.
- A huge amount of pilot symbols should be used to estimate the massive MIMO channels $\mathbf{H}_{b,k}^{[l]}$ (a large matrix), and a huge CSI feedback overhead is involved.
- Global real-time CSIT is required for computing $\mathbf{V}_k^{[b]}$. However, the cross link information $\mathbf{H}_{b,k}^{[l]}$ can only be obtained via message passing among the backhauls connecting the BS. This induces a huge burden on the backhaul and increases the signaling latency.

Remark 1 (Inter-cell Interference in Massive MIMO): It is reported that the inter-cell interference (ICI) of multi-cell massive MIMO systems can be asymptotically ignored [26] using simple per-cell zero-forcing. One key assumption is that the direct links and interference links are spatially uncorrelated. However, such uncorrelation may not hold under local scattering (such as the one-ring scattering model considered in this paper), and hence, ICI coordination may be needed for massive MIMO.

To deal with these challenges, we propose a two-tier precoding in the next section.

III. TWO-TIER PRECODING: JOINT SIGNAL AND INTERFERENCE SUBSPACE ALIGNMENT

In this section, we propose a two-tier precoding structure by exploiting the limited local scattering and the clustering structure of mobile users in cellular systems.

A. Two-tier Precoding with Subspace Alignment

The precoder at BS b to MS k have the two-tier structure given by:

$$\mathbf{V}_k^{[b]} = \mathbf{\Phi}^{[b]} \mathbf{F}_k^{[b]} \quad (5)$$

where $\mathbf{\Phi}^{[b]} \in \mathbb{C}^{N_t \times m_b}$ is the outer subspace precoder that adapts to the large timescale spatial correlations to mitigate the *inter-cell interference*, and $\mathbf{F}_k^{[b]} \in \mathbb{C}^{m_b \times d_{b,k}}$ is the inner precoder that utilizes the real-time local CSIT to mitigate the *intra-cell interference*. The outer precoder $\mathbf{\Phi}^{[b]}$ is computed in a long-timescale once every super-frame, and the inner precoder $\mathbf{F}_k^{[b]}$ (and the corresponding receiver shaping matrices $\mathbf{U}_{b,k}$) is computed in a short-timescale once every subframe. The parameter m_b determines the dimension of the subspace for intra-cell spatial multiplexing. In the massive MIMO scenario, we have $m_b \ll N_t$.

Specifically, the *two-tier precoding with subspace alignment* is described below:

- **Long-Timescale Processing:** In each super-frame, the subspace precoders $\{\Phi^{[b]}\}_{b=1}^G$ are chosen as the solution to the following optimization problem

$$\min_{\{\Phi^{[b]}\}} \underbrace{\sum_{l,b,k,l \neq b} \mathbb{E} \left\| \mathbf{H}_{b,k}^{[l]} \Phi^{[l]} \right\|_F^2}_{\text{inter-cell interference}} - w \underbrace{\sum_{b,k} \mathbb{E} \left\| \mathbf{H}_{b,k}^{[b]} \Phi^{[b]} \right\|_F^2}_{\text{intra-cell signal energy}} \quad (6)$$

subject to $\Phi^{[b]\dagger} \Phi^{[b]} = \mathbf{I}_{m_b}$, where the expectations are conditioned on the spatial correlation matrices $\{\mathbf{T}_{b,k}^{[l]}\}$ and $w > 0$ is a weight parameter.

Remark 2: Minimizing the first term in (6) only corresponds to the conventional ZF solution. Whereas, minimizing the second term alone corresponds to the match filter (MF) solution. The formulation (6) is to strike a balance between the inter-cell interference leakage and the intra-cell signal energy in a system with a large but finite number of antennas. On one hand, for large number of transmit antennas, the second term dominates and the solution approaches the MF solution. On the other, for limited number of antennas (such as traditional MIMO), the first term is significant and the solution approaches the coordinated ZF solution. The weight w is to adjust the balance between the inter-cell interference and the direct link signal.

- **Short-Timescale Processing:** In each subframe, a ZF precoding [23] is used.

Step 1: Choose the receiver shaping matrix $\mathbf{U}_{b,k} \in \mathbb{C}^{N_r \times d_{b,k}}$ for MS k in cell b by solving

$$\min_{\{\mathbf{U}_{b,k}\}} \underbrace{\sum_{l \neq b} \left\| \mathbf{U}_{b,k}^\dagger \mathbf{H}_{b,k}^{[l]} \Phi^{[l]} \right\|_F^2}_{\text{remaining inter-cell interference}} - w \underbrace{\left\| \mathbf{U}_{b,k}^\dagger \mathbf{H}_{b,k}^{[b]} \Phi^{[b]} \right\|_F^2}_{\text{direct link signal}} \quad (7)$$

subject to $\mathbf{U}_{b,k}^\dagger \mathbf{U}_{b,k} = \mathbf{I}_{d_{b,k}}$, and feedback the equivalent channel $\hat{\mathbf{H}}_{b,k}^{[b]} = \mathbf{U}_{b,k}^\dagger \mathbf{H}_{b,k}^{[b]} \Phi^{[b]}$ to BS b .

Step 2: Concatenate the rows of $\hat{\mathbf{H}}_{b,k}^{[b]}$ for each MS k to form a $(\sum_k d_{b,k}) \times m_b$ matrix $\tilde{\mathbf{H}}^{[b]} \triangleq [\hat{\mathbf{H}}_{b,1}^{[b]\dagger} \hat{\mathbf{H}}_{b,2}^{[b]\dagger} \dots \hat{\mathbf{H}}_{b,K_b}^{[b]\dagger}]^\dagger$. The inner precoder $\mathbf{F}^{[b]}$ is given by³

$$\mathbf{F}^{[b]} = \sqrt{\frac{P}{d_b}} \tilde{\mathbf{H}}^{[b]\ddagger} = \sqrt{\frac{P}{d_b}} \tilde{\mathbf{H}}^{[b]\dagger} (\tilde{\mathbf{H}}^{[b]} \tilde{\mathbf{H}}^{[b]\dagger})^{-1} \quad (8)$$

where $\tilde{\mathbf{H}}^{[b]\ddagger}$ denotes the *pseudo-inverse* for $\tilde{\mathbf{H}}^{[b]}$. The inner precoder $\mathbf{F}_k^{[b]}$ for MS k is given by the $(\sum_{j=1}^{k-1} d_{b,j} + 1)$ -th to the $(\sum_{j=1}^k d_{b,j})$ -th columns of $\mathbf{F}^{[b]}$.

Remark 3: Similar to the outer precoding, the problem (7) tries to strike a balance between the (remaining) inter-cell interference and the direct link signal. The inner precoder (8) corresponds to the ZF solution in a single cell multiuser MIMO system [23].

³We assume that the number of data streams $d_{b,k}$ assigned to each user always satisfy $\sum_k d_{b,k} \leq m_b$. Hence, with probability 1, the matrix $\tilde{\mathbf{H}}^{[b]}$ has full row rank.

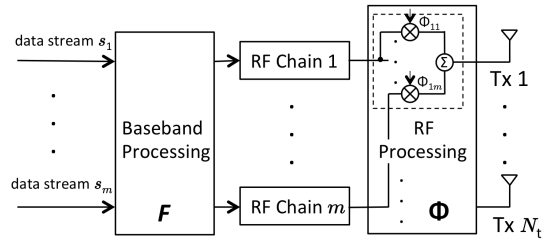


Figure 2. An implementation diagram of the two-tier precoding processing, where only m ($m \ll N_t$) RF chains are used.

B. Motivation of the Two-Tier MIMO Precoding and the Complexity Issue

The two-tier MIMO precoding has the following advantages:

- 1) *A light demand on pilot symbols and CSI feedback overheads:* With the outer precoding, the MS only needs to estimate the $N_r \times m_b$ effective channel $\mathbf{H}_{b,k}^{[b]} \Phi^{[b]}$ and feedback the $d_{b,k} \times m_b$ channel matrix $\mathbf{U}_{b,k}^\dagger \mathbf{H}_{b,k}^{[b]} \Phi^{[b]}$. Instead of directly working on the $N_r \times N_t$ channel matrix $\mathbf{H}_{b,k}^{[b]}$, there is a huge saving on the pilot symbols for channel estimation and the CSI feedback loading.
- 2) *A relatively small number of RF chains required:* With the limited local scattering around the BS, there is only a few active eigen-modes for the massive MIMO channel, and a small number of spatial multiplexing data streams $\sum_k d_{b,k}$ can be supported. Therefore, we do not need to implement N_t RF chains. Instead, only m_b RF chains are required, where $\sum_k d_{b,k} < m_b \ll N_t$ and the outer precoder $\Phi^{[b]}$ can be implemented using the RF phase shifting network [27], [28] as illustrated in Fig. 2.
- 3) *Only statistical global CSI required:* The inner precoder $\mathbf{F}^{[b]}$ only requires the local CSI between the BS and its serving MSs. To update the outer precoder $\Phi^{[b]}$ in the long-timescale, only the knowledge of channel statistics $\mathbb{E} [\mathbf{H}_{l,k}^{[b]\dagger} \mathbf{H}_{l,k}^{[b]}]$ is required. As a result, the performance is insensitive to backhaul latency among the BSs.

Having addressed the practical issues (i)-(iii) raised in Section I, we now focus on the computational complexity issue in (iv). Note that, with the dimension reduction for the inner precoder, the computation for the outer precoder dominates the complexity. We first investigate the solution property for the outer precoding problem (6).

Theorem 1 (Solution to the Outer Precoder): The optimal solution $\Phi_*^{[b]} \in \mathbb{C}^{N_t \times m_b}$ to the outer precoding problem (6) is given by the eigenvectors corresponding to the m_b smallest eigenvalues of the covariance matrix

$$\mathbf{Q}^{[b]} \triangleq \sum_{l \neq b} \sum_{k=1}^{K_l} \mathbb{E} \left(\mathbf{H}_{l,k}^{[b]\dagger} \mathbf{H}_{l,k}^{[b]} \right) - w \sum_{k=1}^{K_b} \mathbb{E} \left(\mathbf{H}_{b,k}^{[b]\dagger} \mathbf{H}_{b,k}^{[b]} \right) \quad (9)$$

for each BS b . ■

Proof: Please refer to Appendix A for the proof. ■

Although Theorem 1 gives a closed form expression for $\Phi^{[b]}$, computing $\Phi^{[b]}$ still require a huge computation complexity of $\mathcal{O}(N_t^3)$. For example, using SVD for the $N_t \times N_t$

covariance matrix $\mathbf{Q}^{[b]}$ requires $\mathcal{O}(N_t^3)$ arithmetic operations. We will address the computation complexity issue in Section IV and V.

C. Achievable Per-cell DoF of Two-Tier Precoding in Massive MIMO

In this section, we characterize the performance of the two-tier precoding by evaluating its achievable DoF per-cell. The DoF can be interpreted as the number of data streams or the asymptotic throughput performance that can be supported in the massive MIMO systems at high SNR [25], [29]. Denote $C_b(P; \{\mathbf{H}_{b,k}^{[l]}\})$ as the sum throughput of cell b . The per-cell DoF of the massive MIMO system is defined as $\Gamma = \frac{1}{G} \sum_{b=1}^G \lim_{P \rightarrow \infty} \frac{C_b(P; \{\mathbf{H}_{b,k}^{[l]}\})}{\log P}$.

For simplicity, we consider a symmetric massive MIMO network, where each cell has the same number of MSs, $K_b = K$, the same rank $\Upsilon_b = \Upsilon < N_t$ of transmit spatial correlation matrices $\mathbf{T}_b^{[l]}$, and $m_b = \min\{\Upsilon, KN_r\}$ for all b . We derive the network DoF of the two-tier precoding in the symmetric massive MIMO system below.

Theorem 2: (Per-cell DoF of Symmetric Massive MIMO Systems with Two-tier Precoding) For a symmetric massive MIMO network $(N_t, N_r, K)^G$, where all the transmit correlation matrices have rank Υ , if $N_t \geq G \max\{\Upsilon, \min\{\Upsilon, KN_r\}\}$, then

- the per-cell DoF of the proposed two-tier precoding is given by $\Gamma_{\text{two}} = \min\{\Upsilon, KN_r\}$,
- the per-cell DoF of conventional one-tier interference alignment (with global real-time CSIT) is given by $\Gamma_{\text{one}} = \min\{\Upsilon, KN_r\}$.

Proof: Please refer to Appendix B for the proof. ■

As a result, there is no loss of DoF performance using the proposed two-tier precoding design in a symmetric multi-cell massive MIMO network⁴.

IV. ITERATIVE ALGORITHMS FOR OUTER PRECODER UNDER TIME-VARYING CHANNELS

To reduce the complexity of finding the global optimal solution for the outer precoder problem in (6), one approach is to leverage on the slowly varying nature of the spatial correlation $\mathbf{T}_b^{[l]}[n]$ and to compute the outer precoder iteratively at every super-frame. A common technique for such iterative outer precoder is to apply the gradient descent algorithm to solve problem (6). However, such a “naive” method may have a poor convergence performance, because problem (6) is non-convex due to the quadratic equality constraints $\mathbf{\Phi}^{[b]\dagger} \mathbf{\Phi}^{[b]} = \mathbf{I}_{m_b}$. Furthermore, problem (6) suffers from uncountably many non-unique and non-isolated local optima. For example, if $\mathbf{\Phi}_*^{[b]}$ is one local optimum, then $\mathbf{\Phi}_*^{[b]} \mathbf{M}$ gives another local optimum, where \mathbf{M} is any unitary matrix. Such a non-isolated property makes it hard to develop

⁴Although the DoF result only focuses on a special network topology region specified by $N_t \geq G \max\{\Upsilon, \min\{\Upsilon, KN_r\}\}$, the region does cover the interested application scenario of massive MIMO systems, since N_t is usually very large and Υ is relatively small in massive MIMO systems.

iterative algorithms with fast convergence to the global optimal solution under time varying channels. Hence, we need to tackle the following challenge,

Challenge 1: To derive a low complexity iterative algorithm which can be shown to converge to the desired solution for the outer precoder $\mathbf{\Phi}^{[b]}$ under time-varying channels.

To deal with the above challenge, we focus on deriving algorithms on the *Grassmann manifold*, where all the outer precoders $\mathbf{\Phi}^{[b]}$ that span the same subspace are considered to be equivalent and are represented by a single point on the Grassmann manifold. As a result, the local optimum becomes isolated.

A. Transformation of Problem (6) on Grassmann Manifold

A *Grassmann manifold* $\text{Grass}(m, N_t)$ is the set of all m -dimensional subspaces of $\mathbb{C}^{N_t \times N_t}$: $\text{Grass}(m, N_t) = \{\text{span}(\mathbf{\Phi}) : \mathbf{\Phi} \in \mathbb{C}^{N_t \times m}, \text{rank}(\mathbf{\Phi}) = m\}$, where $\text{span}(\mathbf{\Phi})$ denotes the space spanned by the columns of the matrix $\mathbf{\Phi}$. The *Grassmann manifold* $\text{Grass}(m, N_t)$ can be considered as a *topology* embedded on the Euclidean space $\mathbb{C}^{N_t \times m}$ with a mapping $\pi : \mathbb{C}^{N_t \times m} \mapsto \text{Grass}(m, N_t)$ that maps each point from the Euclidean space $\mathbb{C}^{N_t \times m}$ to the manifold $\text{Grass}(m, N_t)$. For example, all the matrices $\mathbf{\Phi} \mathbf{M} \in \mathbb{C}^{N_t \times m}$ ($\mathbf{M} \in \mathbb{C}^{m \times m}$ with full rank m), which span the same subspace as $\mathbf{\Phi}$ does, are all mapped to the same element in $\text{Grass}(m, N_t)$ under the mapping π , i.e., $\pi(\mathbf{\Phi}) = \pi(\mathbf{\Phi} \mathbf{M}) \in \text{Grass}(m, N_t)$. On the other hand, the inverse mapping $\pi^{-1}(\mathbf{\Phi})$ represents the set of matrices in the Euclidean space $\mathbb{C}^{N_t \times m}$ that span the same subspace.

Consider $\tilde{\mathbf{\Phi}} = (\mathbf{\Phi}^{[1]}, \dots, \mathbf{\Phi}^{[G]})$ as an element on the Grassmann manifold, i.e., $\tilde{\mathbf{\Phi}} \in \prod_b \text{Grass}(m_b, N_t)$. The outer precoding problem (6) (see equation (23) in Appendix A) can be reformulated as an optimization over the Grassmann manifold [30], [31]

$$\min_{\tilde{\mathbf{\Phi}}} \mathcal{I}(\tilde{\mathbf{\Phi}}) \triangleq \sum_{b=1}^G \text{tr} \left[(\mathbf{\Phi}^{[b]\dagger} \mathbf{\Phi}^{[b]})^{-1} \mathbf{\Phi}^{[b]\dagger} \mathbf{Q}^{[b]} \mathbf{\Phi}^{[b]} \right] \quad (10)$$

where the *global optimal solution* is defined to be the subspace $\tilde{\mathbf{\Phi}}_* \in \prod_b \text{Grass}(m_b, N_t)$ that yields the minimum objective value of (10).

Note that, there is a substantial difference between the formulation (10) in the Grassmann manifold and (6) in the Euclidean space. While the objective in (6) is to find a matrix in the Euclidean space that minimizes the interference and signal utility function \mathcal{I} , the problem (10) focuses on choosing the right subspace $\tilde{\mathbf{\Phi}}_*$, which is a unique solution to minimizing \mathcal{I} ⁵. With this insight, we can derive algorithms to obtain the subspace precoders $\tilde{\mathbf{\Phi}}_*^{[b]}$ more efficiently.

B. Outer Precoder Tracking Algorithm with Compensations

An intuitive way to derive an algorithm that solves the problem (10), is to generalize the gradient descent algorithm to the Grassmann manifold:

$$\tilde{\mathbf{\Phi}}[n+1] = \tilde{\mathbf{\Phi}}[n] + \gamma_n F(\tilde{\mathbf{\Phi}}[n]; \mathcal{Q}[n]) \quad (11)$$

⁵Problem (10) has a unique solution, if, for $b = 1, \dots, G$, the m_b -th eigenvalue of the covariance matrix $\mathbf{Q}^{[b]}$ has multiplicity 1.

where γ_n is the step size, and

$$F(\tilde{\Phi}; \mathcal{Q}) \triangleq \nabla \mathcal{I}(\tilde{\Phi}; \mathcal{Q}) \quad (12)$$

is the gradient iteration mapping on the Grassmann manifold and $\mathcal{Q}[n] = (\mathbf{Q}^{[1]}[n], \dots, \mathbf{Q}^{[G]}[n])$ is a collection of the covariance matrices at iteration n . The notation $\mathcal{I}(\tilde{\Phi}; \mathcal{Q})$ emphasizes that \mathcal{Q} is the key parameter that determines the optimal solution $\tilde{\Phi}_*(\mathcal{Q})$.

Although the gradient descent algorithm usually finds a stationary point under static parameters, it may not be the case under the time-varying parameter $\mathcal{Q}[n]$. Under time-varying channels, the channel covariance matrices $\{\mathbf{Q}^{[b]}[n]\}$ are varying in a similar timescale as the gradient iterations and there is always a convergence gap between the gradient iterate $\tilde{\Phi}[n]$ and the time-varying optimal solution $\tilde{\Phi}_*(\mathcal{Q}[n])$. Taking the precoder $\Phi^{[b]}$ for BS b as an example: When the gradient iteration $\tilde{\Phi}^{[b]}[n+1]$ gets closer to the previous target $\tilde{\Phi}_*^{[b]}[n]$ at the $(n+1)$ -th iteration, the optimal target has already moved to a new position $\tilde{\Phi}_*^{[b]}[n+1]$, which contributes to an additional tracking error.

Intuitively, one way to enhance the tracking of the outer precoder under time-varying channels is to estimate the motion of the moving target $\tilde{\Phi}_*^{[b]}[n]$ and compensate for it:

$$\tilde{\Phi}[n+1] = \tilde{\Phi}[n] + \gamma_n F(\tilde{\Phi}[n]; \mathcal{Q}[n]) + \Delta \widehat{\tilde{\Phi}_*^{[b]}[n]} \quad (13)$$

where the compensation term $\Delta \widehat{\tilde{\Phi}_*^{[b]}[n]}$ is an estimation of the difference of $\tilde{\Phi}_*^{[b]}[n+1] - \tilde{\Phi}_*^{[b]}[n]$.

In the following, we illustrate how to derive the gradient mapping $F(\cdot)$ and the compensation term $\Delta \widehat{\tilde{\Phi}_*^{[b]}[n]}$.

1) *Gradient on the Grassmann Manifold:* Using calculus on Grassmann manifolds [31], [32], the gradient of $\mathcal{I}(\tilde{\Phi})$ in (12) can be derived from $\nabla \mathcal{I} = \mathcal{P}_{\tilde{\Phi}} \bar{\nabla} \mathcal{I}(\tilde{\Phi})$, where $\bar{\nabla} \mathcal{I}(\tilde{\Phi})$ is the gradient of $\mathcal{I}(\tilde{\Phi})$ on the Euclidean space and $\mathcal{P}_{\tilde{\Phi}}$ is to project $\bar{\nabla} \mathcal{I}(\tilde{\Phi})$ onto the *tangent space* [32] of $\tilde{\Phi}$ on the Grassmann manifold. Moreover, it is observed that, there is no cross product of $\Phi^{[b]}$ and $\Phi^{[b]}$ in $\mathcal{I}(\tilde{\Phi})$, and hence we can compute $F^{[b]}(\Phi^{[b]}; \mathbf{Q}^{[b]}) \triangleq \nabla_{\Phi^{[b]}} \mathcal{I}(\tilde{\Phi}; \mathcal{Q})$ separately. As a result, the gradient $\nabla \mathcal{I}$ is given by $F(\tilde{\Phi}; \mathcal{Q}) = (F^{[1]}(\Phi^{[1]}; \mathbf{Q}^{[1]}), \dots, F^{[G]}(\Phi^{[G]}; \mathbf{Q}^{[G]}))$, where $F^{[b]}(\Phi^{[b]}; \mathbf{Q}^{[b]})$ is the partial derivative w.r.t. the precoder $\Phi^{[b]}$, $b = 1, \dots, G$,

$$F^{[b]}(\Phi^{[b]}; \mathbf{Q}^{[b]}) = \underbrace{[\mathbf{I} - \Phi^{[b]}(\Phi^{[b]\dagger} \Phi^{[b]})^{-1} \Phi^{[b]\dagger}]}_{\text{Projection } \mathcal{P}_{\Phi^{[b]}}} \underbrace{\mathbf{Q}^{[b]} \Phi^{[b]}}_{\text{Gradient } \nabla_{\Phi^{[b]}} \mathcal{I}} \quad (14)$$

2) *Derivation of the Compensation:* Consider the parameter $\mathcal{Q}[n]$ in (10) as a discrete-time sampling of the continuous-time covariance matrix profile $\mathcal{Q}(t)$. The *optimality condition* [33], [34] of problem (10) on the Grassmann manifold $\prod_b \text{Grass}(m_b, N_t)$ is given by:

$$F(\tilde{\Phi}_*; \mathcal{Q}(t)) = \mathbf{0}. \quad (15)$$

Note that, since the function $\nabla \mathcal{I}(\cdot)$ is nonlinear, we cannot easily solve (15) to get $\tilde{\Phi}_*(\mathcal{Q}(t))$. However, we are only interested in the differential $d\tilde{\Phi}_*$.

Taking the differentiation on (15) w.r.t. t , we get

$$\text{Hess}_{\tilde{\Phi}_*}(d\tilde{\Phi}_*) + F(\tilde{\Phi}_*; d\mathcal{Q}(t)) = \mathbf{0} \quad (16)$$

where $F(\tilde{\Phi}_*; d\mathcal{Q}(t)) \triangleq F(\tilde{\Phi}_*; \mathcal{Q}(t+dt)) - F(\tilde{\Phi}_*; \mathcal{Q}(t))$ is the partial differential of $F(\tilde{\Phi}_*; \mathcal{Q}(t))$ on the covariance matrix profile $\mathcal{Q}(t)$, and $\text{Hess}_{\tilde{\Phi}_*}(d\tilde{\Phi}_*)$ is the partial differential of $F(\tilde{\Phi}_*; \mathcal{Q}(t))$ on $\tilde{\Phi}_*$ on the Grassmann manifold $\prod_b \text{Grass}(m_b, N_t)$ along the direction $d\tilde{\Phi}_*$. Note that as the function $F(\cdot)$ in (15) is the gradient of the objective function $\mathcal{I}(\tilde{\Phi})$ in (10), $\text{Hess}_{\tilde{\Phi}_*}(d\tilde{\Phi}_*)$ represents the Hessian of $\mathcal{I}(\tilde{\Phi})$.

Consider the case that the optimal solution $\tilde{\Phi}_*$ is non-degenerate, i.e., the function $F(\tilde{\Phi}_*; \mathcal{Q}(t)) = \mathbf{0}$ in (15) has a unique solution over the neighborhood of $\tilde{\Phi}_*$. By the *implicit function theorem* [32], the linear equation (16) has a unique solution $d\tilde{\Phi}_* = \xi$. Consider that the outer precoder $\tilde{\Phi}$ obtained from the previous iteration is already a good approximation of $\tilde{\Phi}_*$, and the fact that the objective function $\mathcal{I}(\tilde{\Phi}; \mathcal{Q})$ is decoupled on each component $\Phi^{[b]}$, we can estimate the differential $d\tilde{\Phi}_*$ by $\hat{\xi} = (\hat{\xi}^{[1]}, \dots, \hat{\xi}^{[G]})$, where $\xi^{[b]}$, $b = 1, \dots, G$, is obtained by solving (17) for $\xi^{[b]}$,

$$\text{Hess}_{\Phi^{[b]}}(\hat{\xi}^{[b]}) + F^{[b]}(\Phi^{[b]}; d\mathbf{Q}^{[b]}(t)) = \mathbf{0}. \quad (17)$$

3) *Low Complexity Calculation on Grassmann Manifold for the Compensation Term:* Although the compensation equation (17) is linear in the matrix variable $\hat{\xi}$, it is a *Sylvester equation* in the general form $\mathbf{A}\hat{\xi} + \hat{\xi}\mathbf{B} + \mathbf{C} = \mathbf{0}$, which is difficult to solve. However, using the property that $\hat{\xi}$ is a point on the Grassmann manifold, we can find a low complexity algorithm to solve the compensation equation (17).

Consider $\Phi^{[b]}$ are already orthonormalized. Using the calculus on the Grassmann manifold [31], [35], the term $\text{Hess}_{\Phi^{[b]}}(\hat{\xi}^{[b]})$ can be derived as

$$\begin{aligned} & \text{Hess}_{\Phi^{[b]}}(\hat{\xi}^{[b]}) \\ &= \mathcal{P}_{\Phi^{[b]}} \left\{ \lim_{t \rightarrow 0} \left[F(\Phi_*^{[b]} + t\hat{\xi}^{[b]}; \mathcal{Q}) - F(\Phi_*^{[b]}; \mathcal{Q}) \right] \right\} \\ &= \mathcal{P}_{\Phi^{[b]}} \left(\mathbf{Q}^{[b]} \hat{\xi}^{[b]} - \hat{\xi}^{[b]} \Phi^{[b]\dagger} \mathbf{Q}^{[b]} \Phi^{[b]} \right) \end{aligned} \quad (18)$$

Notice that $F^{[b]}(\Phi^{[b]}; d\mathbf{Q}^{[b]}(t))$ is linear in $\Phi^{[b]}$ (c.f. (14)). Multiplying (17) with a unitary matrix \mathbf{M} on the right, we obtain

$$\mathcal{P}_{\Phi^{[b]}} \left[\mathbf{Q}^{[b]} (\hat{\xi}^{[b]} \mathbf{M}) - (\hat{\xi}^{[b]} \mathbf{M}) \underbrace{\mathbf{M}^\dagger \Phi^{[b]\dagger} \mathbf{Q}^{[b]} \Phi^{[b]} \mathbf{M}}_{\Psi} \right] - F^{[b]}(\Phi^{[b]} \mathbf{M}; \mathbf{Q}^{[b]}) = \mathbf{0} \quad (19)$$

where \mathbf{M} diagonalizes $\Phi^{[b]\dagger} \mathbf{Q}^{[b]} \Phi^{[b]}$, i.e., $\Phi^{[b]\dagger} \mathbf{Q}^{[b]} \Phi^{[b]} = \mathbf{M} \Psi \mathbf{M}^\dagger$ and $\Psi = \text{diag}(\beta_1, \dots, \beta_{m_b})$. Let $\mathbf{Y} = \hat{\xi}^{[b]} \mathbf{M}$. Since Ψ is diagonal, equation (19) can be written into m_b parallel linear matrix equations according to each column of \mathbf{Y} ,

$$\mathcal{P}_{\Phi^{[b]}} \left(\mathbf{Q}^{[b]} - \beta_i \mathbf{I} \right) \mathbf{Y}^i + F^{[b]}(\Phi^{[b]} \mathbf{M}; d\mathbf{Q}^{[b]})^i = \mathbf{0} \quad (20)$$

where $i = 1, \dots, m_b$, \mathbf{Y}^i and $F^{[b]}(\Phi^{[b]}; d\mathbf{Q}^{[b]})^i$ are the i -th ($1 \leq i \leq m_b$) columns of \mathbf{Y} and $F^{[b]}(\Phi^{[b]} \mathbf{M}; d\mathbf{Q}^{[b]})$, respectively. The above linear equation can be solved by the *conjugate gradient* (CG) algorithm, which only has complexity of $\mathcal{O}(N_t^2)$.

Algorithm 1 Compensation algorithm for the outer precoding
 During each super-frame n , each MS k in the b -th cell estimates the interference covariance matrix $\mathbf{Q}_{b,k}^{[l]}[n] \triangleq \mathbb{E} \left[\mathbf{H}_{b,k}^{[l]} \mathbf{H}_{b,k}^{[l]\dagger} \right]$. Each BS b updates $\mathbf{Q}^{[b]}[n]$ according to (9) and computes the new outer precoder $\Phi^{[b]}[n+1]$ according to the following steps:

Step 1: Compute the compensation estimator

- 1) ($2m_b N_t^2$ op.) Let $\Delta_n F^{[b]} = F^{[b]}(\Phi_{n-1}^{[b]}; \mathbf{Q}_{n-1}^{[b]}) - F^{[b]}(\Phi_{n-1}^{[b]}; \mathbf{Q}_{n-1}^{[b]})$, where $F^{[b]}(\cdot)$ is given in (14).
- 2) ($2m_b N_t^2$ op.) Find the eigen factorization for the dimension reduced matrix $\Phi_{n-1}^{[b]\dagger} \mathbf{Q}_{n-1}^{[b]} \Phi_{n-1}^{[b]} = \mathbf{M} \Psi \mathbf{M}^*$, where $\Psi = \text{diag}(\beta_1, \dots, \beta_{m_b})$.
- 3) ($6m_b N_t^2$ op.) Compute the coefficient matrix $\mathbf{A}_i^{[b]} = (\mathbf{I} - \Phi_{n-1}^{[b]} \Phi_{n-1}^{[b]\dagger}) (\mathbf{Q}_{n-1}^{[b]} - \beta_i \mathbf{I})$.
- 4) ($4m_b N_t^2$ op.) Solve the equation for \mathbf{Y}^i using CG algorithm with $N_{CG} = 1$ step,

$$\mathbf{A}_i^{[b]} \mathbf{Y}^i + (\Delta_n F^{[b]})^i = \mathbf{0}, \quad \text{for } 1 \leq i \leq m_b.$$

- 5) Update the compensation $\Phi_{(1)}^{[b]} \leftarrow \Phi_{n-1}^{[b]} + \mathbf{Y} \mathbf{M}^*$.

Step 2: ($2m_b N_t^2$ op.) Compute the search direction $\boldsymbol{\eta}^{[b]} = \mathbf{Q}_n^{[b]} \Phi_{(1)}^{[b]}$, for $b = 1, \dots, G$.

Step 3: Update $\Phi_{n+1}^{[b]} \leftarrow \text{qr}(\Phi_{(1)}^{[b]} - \gamma \boldsymbol{\eta}^{[b]})$, where $\gamma > 0$ is the step size and $\text{qr}(\mathbf{A})$ denotes the Gram-Schmidt procedure for the orthogonalization of \mathbf{A} .

C. Complexity and Implementation Considerations

1) *Computational Complexity:* The computational complexity of the proposed compensation algorithm (13) is mainly contributed by the gradient term $F(\Phi[n]; \mathbf{Q}[n])$ and the compensation term $\Delta \widehat{\Phi}_*^{[b]}[n]$ in (13). The gradient term requires $2m_b N_t^2$ (omitting the small order terms) arithmetic operations (addition, multiplication, etc.). The compensation term requires solving the linear equations in (20) with the CG algorithm. Note that, as the CG algorithm has a fast convergence rate and the norm of $F(\Phi; d\mathbf{Q})$ is usually small (since $d\mathbf{Q}$ is small due to the slow time-varying property of the covariance matrix $\mathbf{Q}^{[b]}(t)$), computing only $N_{CG} = 1$ step (requires $4m_b N_t^2$ operations) to obtain $\xi^{[b],i}$ is sufficient to yield a good compensation $\Delta \widehat{\Phi}_*^{[b]}(n)$. Therefore, the proposed compensation algorithm (summarized in Algorithm 1) has a total computational complexity of around $16m_b N_t^2$ operations. As we discussed in Section III-B, we usually have $m_b \ll N_t$ for massive MIMO channels, and therefore the complexity of the proposed algorithm is substantially lower than $\mathcal{O}(N_t^3)$ of the brute force computing of Theorem 1 using SVD [36].

2) *Implementation Considerations:* Fig. 3 gives a diagram of the associated signaling for the two-tier precoding. In stage (a), each BS b broadcasts channel training sequences using the outer precoder $\Phi^{[b]}$ at each subframe. In stage (b), each MS feeds back the low dimensional equivalent channel at each subframe and full dimension $(N_t \times N_t)$ interference covariance matrices $\{\mathbf{Q}_{b,k}^{[l]}\}$ only at the end of each super-frame. In stage (c), BSs exchange the covariance matrix profile $\{\mathbf{Q}_{b,1}^{[l]}\}$ for

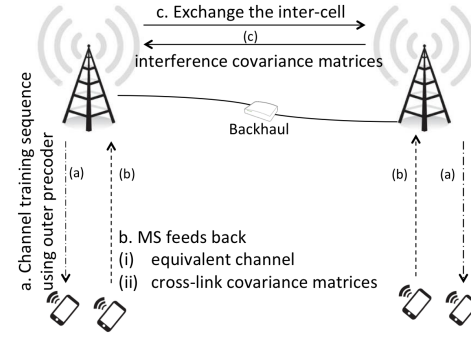


Figure 3. Diagram of the signaling in the multi-cell massive MIMO system.

each MS cluster through the backhaul only at the end of each super-frame. As a result, the pilot symbols for channel estimation, the CSI feedback overhead and the signaling over the backhaul have been greatly reduced in the massive MIMO system.

V. CONVERGENCE ANALYSIS OF THE OUTER PRECODING ALGORITHM

In this section, we analyze the tracking performance of the proposed iterative outer precoder tracking algorithms under time-varying channels. We are interested in whether algorithm (13) will converge to the global optimal solution of the problem in (6). However, since the problem in (6) is non-convex and there are multiple stationary points for the algorithm, existing techniques [37], [38] for the convergence analysis under time-varying channels cannot be applied. In general, we shall address the following challenge:

Challenge 2: Analyze the convergence behavior for the outer precoder tracking algorithm under the time-varying massive MIMO channel, despite the optimization problem being non-convex.

Towards this end, we extend the analysis framework in [37], [38] and obtain the results of the algorithm tracking performance by analyzing an equivalent continuous-time virtual dynamic system (VDS), which models the behavior of the algorithm iteration. Please refer to Appendix C for details.

A. Convergence under Static Channel Covariance

When the channel covariance matrices $\mathbf{Q}^{[b]}$ are static, the compensation term in iteration (13) is always zero. Hence, the compensation algorithm (13) degenerates to a pure gradient descent algorithm (11). To establish the convergence results, we first derive the following uniqueness property for the algorithm.

Lemma 1 (Uniqueness of Global Optimal Point): Suppose under a given $\mathcal{Q} = (\mathbf{Q}^{[1]}, \dots, \mathbf{Q}^{[G]})$, the covariance matrix $\mathbf{Q}^{[b]}$ has distinct m_b -th and $(m_b + 1)$ -th smallest eigenvalues $\lambda_{m_b}^{[b]} \neq \lambda_{m_b+1}^{[b]}$ for each b . Then there is only one global optimal stationary point for the iteration (13). ■

Proof: Please refer to Appendix C for the proof. ■

Based on Lemma 1, we shall establish the global convergence result below.

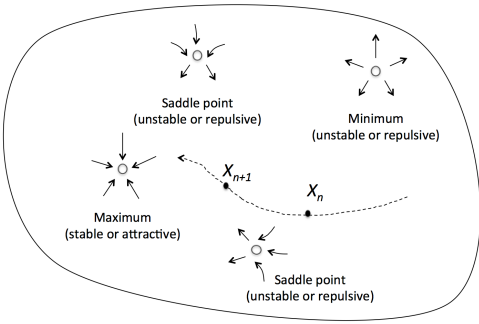


Figure 4. An illustration of the KKT points of problem (10) on the Grassmann manifold. Except for the global maximum point, other KKT points (stationary points or minimum point) are unstable (repulsive).

Theorem 3: (Global Convergence under Static Channel Covariance) There exists $\gamma_0 > 0$, such that under the distinct eigenvalue condition in Lemma 1 and choosing step size $0 < \gamma < \gamma_0$, the proposed algorithm converges to the global optimal solution $\tilde{\Phi}_*(\mathcal{Q})$. ■

Proof: Please refer to Appendix C for the proof. ■

The above theorem concludes that, although the original outer precoding problem (6) is non-convex, the proposed algorithm is guaranteed to converge to the global optimal solution under static channel covariance.

Remark 4 (Global Convergence of Non-Convex Problem):

As we pointed out in Section IV-A, problem (6) is non-convex. Yet, after the problem reformation, the new problem in (10) on the manifold has the following structure: there is only one maximum point (attractive) among all the other KKT points (repulsive) as illustrated in Fig. 4. As a result, the iterative algorithm trajectory will converge to the maximum point almost surely.

B. Convergence under Time-Varying Channel Covariance

We now study the case under time-varying channel covariance. Under time-varying channels, the global optimal solution $\tilde{\Phi}^*(t)$ is also time varying in similar timescale as the algorithm iteration (13) and hence, it is not clear if the iterate $\tilde{\Phi}[n]$ can converge to $\tilde{\Phi}^*(t_n)$.

To analyze the tracking performance of the outer precoder iterations in (13), we approximate the discrete-time iterations $\tilde{\Phi}[n]$ with the following continuous time iterations⁶ $\tilde{\Phi}^c(t)$, which is defined as the solution of the following differential equations:

$$d\tilde{\Phi}^c = F(\tilde{\Phi}^c; \mathcal{Q}(t))dt + d\tilde{\Phi}^c, \quad \tilde{\Phi}^c(0) = \tilde{\Phi}_0 \quad (21)$$

$$\mathbf{0} = \text{Hess}_{\tilde{\Phi}^c}(d\tilde{\Phi}^c) + F(\tilde{\Phi}^c; d\mathcal{Q}(t)). \quad (22)$$

We evaluate the tracking behavior of the outer precoder iteration $\tilde{\Phi}^c(t)$ in the following.

Theorem 4: (Convergence of the Outer Precoder Iteration in Time-varying Channels) Assume the distinct eigenvalue

⁶The iteration $\tilde{\Phi}[n]$ of (13) is a discretization of the compensated virtual dynamic system $\tilde{\Phi}^c(t)$ at $t = n\tau T_s$ (for example, by replacing dt in (21) with $\gamma_n \approx \Delta t_n$ in (13)).

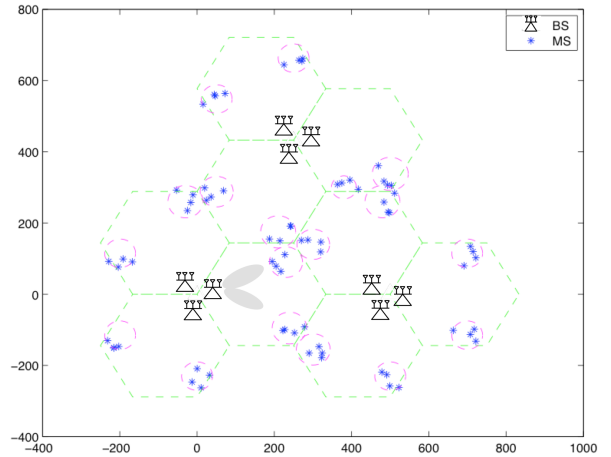


Figure 5. Topology of a cellular network with clusters of users.

condition in Lemma 1. In addition, suppose the largest eigenvalue λ_{\max} of $\mathbf{Q}^{[b]}$ is bounded w.p.1 for all b . Then there exists $\delta > 0$, such that for $\|\tilde{\Phi}^c(0) - \tilde{\Phi}_*(0)\|_F < \delta$, we have $\|\tilde{\Phi}^c(t) - \tilde{\Phi}_*(t)\|_F \rightarrow 0$, w.p.1, as $t \rightarrow \infty$. ■

Proof: Please refer to Appendix D for the proof. ■

The result in Theorem 4 implies that perfect tracking of the outer precoder in time-varying channels is possible if the initial iterate $\tilde{\Phi}[0]$ is sufficiently close to the global optimal point $\tilde{\Phi}_*(0)$.

VI. NUMERICAL RESULTS

We consider a cellular network with $G = 9$ cells, where each cell has 2 clusters and each cluster has $K = 4$ users. Fig. 5 illustrates a realization of the network topology. The inter-site distance is 500 m. The large-scale propagation follows the outdoor evaluation methodology in LTE standard [39] with pathloss exponent 2.6. Each BS is equipped with $N_t = 48$ antennas and each user is equipped with $N_r = 1$ antenna. We generate the massive MIMO channels according to (3), where the transmit correlation matrices are specified by (2) and the AS parameter is modeled as $\Delta_{b,k}^{[l]} = 20$ deg. Moreover, the small timescale channel variation $\mathbf{H}_k^\omega(j)$ in (3) is modeled by the widely used autoregressive (AR) model [40] given by $\mathbf{H}_k^\omega(j) = \theta \mathbf{H}_k^\omega(j-1) + \sqrt{1-\theta^2} \mathbf{W}$, where \mathbf{W} is a standard complex Gaussian matrix, $\theta = J_0(2\pi f_d \tau)$ is the temporal correlation coefficient, $J_0(\cdot)$ is the zero-th order Bessel function, f_d is the maximum Doppler frequency, and $\tau = 1$ is the subframe duration. The length of the super-frame is $T_s = 100$. The noise is normalized as equal to the smallest direct link power gain.

We consider the following baselines: **Baseline 1 (One-tier coordinated MIMO using ZF [23]):** In each subframe, full CSI is used to compute the precoder, which zero-forces both the inter-cell and intra-cell interference. **Baseline 2 (Two-tier precoding using the BD algorithm in [8]):** Two-tier precoding strategy in [8] is applied, where the outer precoder is computed by the BD algorithm in [8]. **Baseline 3 (Two-tier precoding with conventional gradient algorithm for the outer precoder [13]):** The two-tier precoding strategy

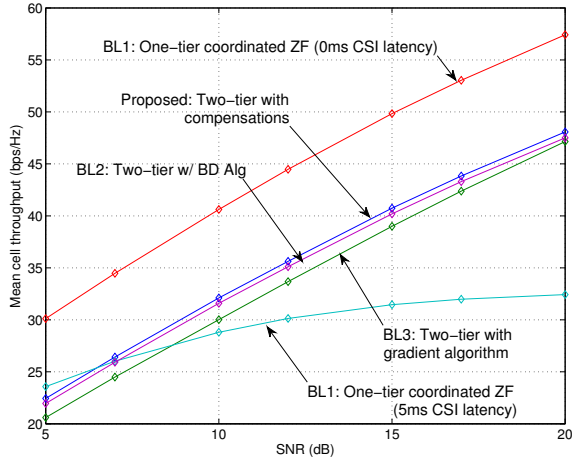


Figure 6. The per cell throughput versus the per BS transmit power under MS speed 10 km/h.

(equations (6), (7) and (8)) is applied, where the solution of the outer precoders given in Theorem 1 are computed iteratively using the gradient algorithm in [13].

Note that Baseline 1 suffers from implementation challenges in massive MIMO systems, such as huge pilot symbols and feedback overhead, and real-time global CSI sharing as discussed in Section I. Hence it serves as performance benchmark only.

A. Throughput Performance

Fig. 6 shows the per cell throughput versus the per BS transmit power under MS speed 10 km/h. The one-tier cooperative ZF scheme (Baseline 1) achieves the highest data rate when there is no signaling latency for the BSs to exchange global CSI over the backhaul. However, the performance of Baseline 1 is very sensitive to the signaling latency and its performance degrades significantly when 5 ms backhaul latency is considered⁷. On the other hand, the performance of the two tier precoding schemes (Baseline 2, Baseline 3 and proposed scheme) are robust to signaling latency, as they do not require instantaneous global CSI. The proposed scheme achieves slightly better performance compared with Baseline 2 but with substantially lower complexity (Table II).

Fig. 7 shows the per cell throughput versus the MS speed under per BS transmit power budget $P = 10$ dB. Similarly, the proposed scheme with compensation achieves good performance but with substantially lower complexity. In addition, it significantly outperforms Baseline 3 at high MS speed. This confirms the superior tracking capability of the proposed compensation algorithm under time-varying channels. As a comparison, the throughput performance of Baseline 1 drops quickly when increasing the MS speed under 5 ms backhaul latency.

⁷As a benchmark, the X2 interface in e-Node B of LTE systems usually induce 10-20 ms latency [39].

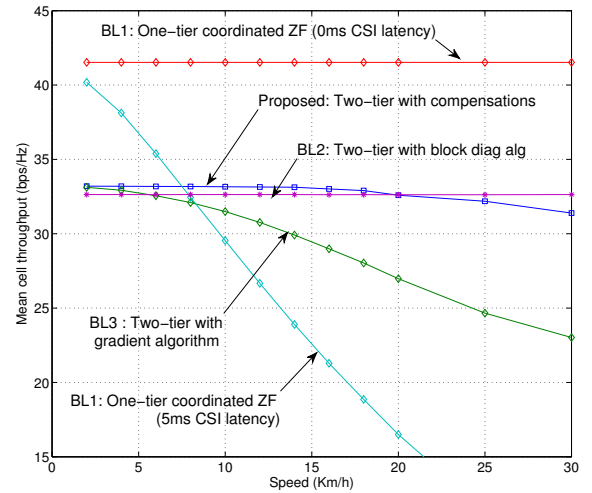


Figure 7. The per cell throughput versus the MS mobility under per BS transmit power $P = 10$ dB.

(N_t, K)	Feedback amount		Signaling loading	
	BL 1	BL 2, 3 & Prop	BL 1	BL 2, 3 & Prop
	$N_t N_r K$	$N_t^2 / T_s + N_r K^2$	$3N_t N_r K$	$3N_t^2 / T_s$
(24, 8)	384	134	1,152	17
(48, 8)	768	151	2,304	69
(100, 30)	6,000	1,900	18,000	300

Table I

AVERAGE CSI FEEDBACK AMOUNT AND SIGNALING LOADING IN TERMS OF NUMBER OF COMPLEX NUMBERS PER CELL PER SUBFRAME, WHERE $N_r = 2$, THE DIMENSION OF THE OUTER PRECODER IS $m = K$, $T_s = 100$, AND ONE CLUSTER PER CELL.

B. Feedback Loading and Complexity

Table I shows numerical examples of CSI feedback amount and signaling loading in terms of number of complex numbers per cell per subframe following the discussion in Section IV-C2. We assume each cell only needs to exchange CSI to 3 neighboring cells. Baseline 1 requires a high feedback cost and signaling loading. Whereas, the proposed scheme has significantly lowered the CSI feedback overhead among BSs in massive MIMO systems.

Table II summarizes the computational complexity⁸ in terms of the millions of complex multiply-accumulate (MCM) operations per super-frame and the corresponding computational time⁹ for computing the outer precoder for one cluster under a two-tier precoding strategy. The proposed algorithm has a much lower complexity than the BD algorithm (Baseline 2) and the scheme using the brute force computation of Theorem 1.

VII. CONCLUSIONS

In this paper, we propose a low complexity compensation algorithm for tracking the outer precoder under the two-tier

⁸The major complexity of these algorithms consists for the complexity of pseudo inverse (from ZF solution) [41] and the complexity of eigen analysis.

⁹The computational time is estimated by using a TI-TMS320DM642 DSP, which can execute up to 4800 million instructions per second (MIPS). Operation overheads such as memory loading are not counted.

(N_t, K)	MCMA & time (ms)		
	BD (BL 2)	SVD	Proposed
	$21N_t^3 + 21(N_t - r^*)^3$	$21N_t^3$ [36]	$16mN_t^2$
(24, 8)	0.37 (0.078)	0.29 (0.06)	0.07 (0.02)
(48, 8)	3.67 (0.76)	2.3 (0.48)	0.29 (0.06)
(100, 8)	37 (7.8)	21 (4.4)	1.3 (0.27)

Table II

ROUGH CALCULATION OF THE COMPUTATIONAL COMPLEXITY IN TERMS OF MILLIONS OF COMPLEX MULTIPLY-ACCUMULATE (MCMA) OPERATIONS PER SUPER-FRAME AND THE CORRESPONDING COMPUTATIONAL TIME IN MILLISECONDS USING TI-TMS320DM642 DSP FOR COMPUTING THE OUTER PRECODER FOR ONE CLUSTER. THE DIMENSION OF THE OUTER PRECODER FOR THE PROPOSED SCHEME IS CHOSEN AS $m = r^* = K$.

precoding in massive MIMO systems and time-varying channels. The two-tier precoding scheme tries to combat various implementation challenges raised in massive MIMO systems, namely, the huge pilot symbols and feedback overhead, real-time global CSI requirement, large number of RF chains and high computational complexity. In particular, to reduce the computational complexity for the outer precoder, we propose an iterative algorithm which is derived by solving an optimization problem formulated on the Grassmann manifold, and its tracking performance is enhanced by leveraging a compensation technique to offset the time variation of the optimal solution. We show with analytical results that, under some mild conditions, perfect tracking of the outer precoder is possible. The numerical results also confirm the superior performance advantage of the two-tier precoding with the proposed compensation algorithm.

APPENDIX A

PROOF OF THEOREM 1

Denote $\tilde{\Phi} = (\Phi^{[1]}, \dots, \Phi^{[G]})$ as the subspace precoder profile for all the BSs. The objective function in the outer precoding problem in (6) can be written as

$$\begin{aligned}
\mathcal{I}(\tilde{\Phi}) &\triangleq \sum_{b=1}^G \sum_{l \neq b} \sum_{k=1}^{K_l} \text{tr} \left[\mathbb{E} \left(\mathbf{H}_{b,k}^{[l]} \Phi^{[l]} \Phi^{[l]\dagger} \mathbf{H}_{b,k}^{[l]\dagger} \right) \right] \\
&\quad - w \sum_{b=1}^G \sum_{k=1}^{K_l} \text{tr} \left[\mathbb{E} \left(\mathbf{H}_{b,k}^{[b]} \Phi^{[b]} \Phi^{[b]\dagger} \mathbf{H}_{b,k}^{[b]\dagger} \right) \right] \\
&= \sum_{b=1}^G \text{tr} \left\{ \Phi^{[b]\dagger} \left[\sum_{l \neq b} \sum_{k=1}^{K_l} \mathbb{E} \left(\mathbf{H}_{l,k}^{[b]\dagger} \mathbf{H}_{l,k}^{[b]} \right) \right. \right. \\
&\quad \left. \left. - w \sum_{k=1}^{K_b} \mathbb{E} \left(\mathbf{H}_{b,k}^{[b]\dagger} \mathbf{H}_{b,k}^{[b]} \right) \right] \Phi^{[b]} \right\} \\
&= \sum_{b=1}^G \text{tr} \left\{ \Phi^{[b]\dagger} \mathbf{Q}^{[b]} \Phi^{[b]} \right\}
\end{aligned}$$

which is equivalent to solving the following minimization problem

$$\min_{\{\Phi^{[b]\dagger} \Phi^{[b]} = \mathbf{I}_{m_b}\}} \mathcal{I}(\tilde{\Phi}) = \sum_{b=1}^G \text{tr} \left\{ \Phi^{[b]\dagger} \mathbf{Q}^{[b]} \Phi^{[b]} \right\}. \quad (23)$$

Applying eigenvalue decomposition (EVD) to $\mathbf{Q}^{[b]}$, we get $\mathbf{Q}^{[b]} = \mathbf{W}^{[b]} \mathbf{\Lambda}^{[b]} \mathbf{W}^{[b]\dagger}$. Thus due to the unitary constraint

$\Phi^{[b]\dagger} \Phi^{[b]} = \mathbf{I}_{m_b}$, the optimal solution is given by the m_b columns of $\mathbf{W}^{[b]}$ corresponding to the m_b smallest diagonal elements of $\mathbf{\Lambda}^{[b]}$.

APPENDIX B

PROOF OF THEOREM 2

We first consider the outer bound of the DoF Γ_{one} under the one-tier IA. Suppose we allow receiver cooperation in each cluster. As a result, the MIMO interference broadcast channel becomes a G -pair $KN_r \times N_t$ interference channel, and we denote the $KN_r \times N_t$ concatenated channel as $\tilde{\mathbf{H}}_b^{[l]} = [\mathbf{H}_{b,1}^{[l]\dagger}, \dots, \mathbf{H}_{b,K}^{[l]\dagger}]^\dagger$.

Applying EVD to the transmit covariance matrix, we get $\mathbf{T}_b^{[l]} = \mathbf{U}_{T,b}^{[l]} \mathbf{\Lambda}_{T,b}^{[l]} \mathbf{U}_{T,b}^{[l]\dagger} = \sum_{j=1}^\Upsilon \lambda_{b,j}^{[l]} \mathbf{u}_{T,b,j}^{[l]} \mathbf{u}_{T,b,j}^{[l]\dagger}$, where $\mathbf{\Lambda}_{T,b}^{[l]}$ is a diagonal matrix with diagonal elements $\{\lambda_{b,j}^{[l]}\}_{j=1}^\Upsilon$ sorted in a descent order and $\mathbf{u}_{T,b,j}^{[l]}$ is the j -th column of $\mathbf{U}_{T,b}^{[l]}$. From the channel model in (3), we have $\mathbf{H}_{b,k}^{[l]} = \mathbf{H}^w \sum_{j=1}^\Upsilon \sqrt{\lambda_{b,j}^{[l]}} \mathbf{u}_{T,b,j}^{[l]} \mathbf{u}_{T,b,j}^{[l]\dagger} = \sum_{j=1}^\Upsilon \hat{\mathbf{H}}_j^w \mathbf{u}_{T,b,j}^{[l]\dagger}$, where $\hat{\mathbf{H}}_j^w = \sqrt{\lambda_{b,j}^{[l]}} \mathbf{H}^w \mathbf{u}_{T,b,j}^{[l]}$ and each row of $\mathbf{H}_{b,k}^{[l]}$ is a linear combination of the Υ vectors $\{\mathbf{u}_{T,b,j}^{[l]}\}_{j=1}^\Upsilon$. As a result, the concatenated matrix $\tilde{\mathbf{H}}_b^{[l]}$ has rank at most $\min\{\Upsilon, KN_r\}$. Therefore, using the result in [42, Theorem 1], the G -pair $KN_r \times N_t$ rank deficient interference channel has a per-cell DoF $\min\{\Upsilon, KN_r\}$, and thus, we obtain an outer bound $\Gamma_{\text{one}} \leq \min\{\Upsilon, KN_r\}$.

We now derive the inner bound (achievability) of the DoF Γ_{two} under the two-tier precoding. Construct a principal matrix $\hat{\mathbf{U}}_{T,b}^{[l]}$ for the covariance matrix $\mathbf{T}_b^{[l]}$ of each link by extracting the Υ major eigen components, i.e., $\hat{\mathbf{U}}_b^{[l]} = [\mathbf{u}_{T,b,1}^{[l]} \mathbf{u}_{T,b,2}^{[l]} \dots \mathbf{u}_{T,b,\Upsilon}^{[l]}]$, where $\{\mathbf{u}_{T,b,j}^{[l]}\}$ are the major eigen modes of the transmit covariance matrix from BS l to the clustered users in cell b . Construct the principal signal matrix for each BS b as $\hat{\mathbf{U}}_b = [\hat{\mathbf{U}}_b^{[1]} \dots \hat{\mathbf{U}}_b^{[G]}]^\dagger$ with dimension $(G\Upsilon) \times N_t$. Since all the elements of $\hat{\mathbf{U}}_b$ are independent and continuous distributed, $\hat{\mathbf{U}}_b$ has full row rank $G\Upsilon$ under the condition that $N_t \geq G\Upsilon$. As a result, we can find a pseudo-inverse $\hat{\mathbf{U}}_b^\dagger$ of $\hat{\mathbf{U}}_b$, such that $\hat{\mathbf{U}}_b \hat{\mathbf{U}}_b^\dagger = \mathbf{I}_{G\Upsilon}$. This implies that, there exists a $N_t \times \Upsilon$ matrix $\Phi_\Upsilon^{[b]}$ that $\hat{\mathbf{U}}_b^{[b]} \Phi_\Upsilon^{[b]} = \mathbf{I}_\Upsilon$, $\forall b$, and $\hat{\mathbf{U}}_b^{[l]} \Phi_\Upsilon^{[b]} = \mathbf{0}$, $\forall l \neq b$. As a result, we have

$$\text{rank}(\mathbf{T}_b^{[b]} \Phi_\Upsilon^{[b]}) = \Upsilon, \quad \text{and} \quad \mathbf{T}_b^{[l]} \Phi_\Upsilon^{[b]} = \mathbf{0}, \forall l \neq b. \quad (24)$$

Therefore, with probability 1, we have $\text{rank}(\mathbf{H}_{b,k}^{[b]} \Phi_\Upsilon^{[b]}) = \min\{N_r, \Upsilon\}$, $\forall b$, and $\mathbf{H}_{b,k}^{[l]} \Phi_\Upsilon^{[b]} = \mathbf{0}$, $\forall l \neq b$. Hence, the concatenated matrix $\tilde{\mathbf{H}}_b^{[b]} \Phi_\Upsilon^{[b]}$ has row rank $\min\{\Upsilon, KN_r\}$, and by using transmit ZF, $\min\{\Upsilon, KN_r\}$ DoF can be achieved per cell.

Choose the dimension of the outer precoders $\{\Phi^{[b]}\}_{b=1}^G$ as $N_t \times m$, where $m = \min\{\Upsilon, KN_r\}$. Denote $\tilde{\Phi} = (\Phi^{[1]}, \dots, \Phi^{[G]})$. Consider $w = 0$; then the set of optimal solutions $\tilde{\Phi}_*|_{w=0}$ must satisfy the nulling condition in (24) and the optimal value of (6) is 0. Due to the continuity of the objective function (quadratic forms), there exists a ϵ -neighborhood $\mathcal{N}_0(\tilde{\Phi}_*)$ of some $\tilde{\Phi}_*|_{w=0}$, such that we can

find a $\tilde{\Phi} \in \mathcal{N}_0(\tilde{\Phi}_*)$ to satisfy all the subspace alignment conditions in (24). Hence, choosing w sufficiently small, e.g., $w = \mathcal{O}(\frac{1}{\rho})$ under high SNR ρ , the optimal solution $\tilde{\Phi}_*$ to (6) satisfies the condition (24). As a result, it guarantees that $\Gamma_{\text{two}} \geq \min\{\Upsilon, KN_r\}$. As $\Gamma_{\text{two}} \leq \Gamma_{\text{one}}$, we must have $\Gamma_{\text{two}} = \Gamma_{\text{one}} = \min\{\Upsilon, KN_r\}$.

APPENDIX C CONVERGENCE VIA VIRTUAL DYNAMIC SYSTEM MODELING

A. The Virtual Dynamic System (VDS) Modeling and Proof of Lemma 1

We first model the algorithm iteration into a continuous-time virtual dynamic system defined as follows.

Definition 1 (Continuous-time Virtual Dynamic System):

The continuous-time virtual dynamic system (VDS) is defined by the state trajectory $\tilde{\Phi}^c(t)$, which is the solution to the following differential equation

$$d\tilde{\Phi}^c = -F(\tilde{\Phi}^c; \mathcal{Q}(t))dt, \quad \tilde{\Phi}^c(0) = \tilde{\Phi}[0] \quad (25)$$

where $\tilde{\Phi}[0]$ is the initial state chosen in the tracking algorithms. ■

Correspondingly, we have the following notions associated with the continuous-time dynamic system. The *equilibrium* of the dynamic system is defined as the points $\{\tilde{\Phi}_*^c \in \prod_b \text{Grass}(m_b, N_t)\}$ that satisfy $d\tilde{\Phi}^c = 0$. An equilibrium $\tilde{\Phi}_*^c$ is locally *stable* if there exists a neighborhood $\mathcal{N}(\tilde{\Phi}_*^c) \subseteq \prod_b \text{Grass}(m_b, N_t)$, such that for all $\tilde{\Phi}^c(0) \in \mathcal{N}(\tilde{\Phi}_*^c)$, $\tilde{\Phi}^c(t) \rightarrow \tilde{\Phi}_*^c$ as $t \rightarrow \infty$ almost surely (a.s.). In addition, the dynamic system is called *asymptotically stable* if there exists a unique stable equilibrium and for all $\tilde{\Phi}^c(0)$, we have $\tilde{\Phi}^c(t) \rightarrow \tilde{\Phi}_*^c$ as $t \rightarrow \infty$ a.s.

Intuitively, scaling the step size γ and time slot duration τ , the discrete-time iteration $\tilde{\Phi}[n]$ degenerates to its continuous-time counterpart asymptotically as $\tau \rightarrow 0$. Such asymptotic equivalence can be established using the stochastic approximation framework in [38], [43]. Specifically, we summarize the connection in the following (analogue of [38, Theorem 2]).

Lemma 2: (Connection between the Algorithm Iteration and the Continuous-time Dynamic System) Suppose under each static parameter \mathcal{Q} , the dynamic system $\tilde{\Phi}^c(t)$ is stable. In addition, assume the channel variation speed $\|d\mathcal{Q}/dt\|$ is bounded above. Then for $\tau, \gamma \rightarrow 0$ with $\bar{\gamma} = \gamma/\tau \gg 1$, the iterate $\tilde{\Phi}[n]$ converges to the state trajectory $\tilde{\Phi}^c(t)$ of the continuous-time dynamic system (25), i.e., for any $\epsilon > 0$,

$$\lim_{\tau, \gamma \rightarrow 0} \limsup_{n \rightarrow \infty} \Pr \left\{ \|\tilde{\Phi}[n] - \tilde{\Phi}^c(t_n)\| > \epsilon \right\} = 0$$

where $t_n = nT_s\tau$. ■

From the above equivalent connection, proving Lemma 1 for the iteration (13) under static channels is equivalent to showing that there is only one stable equilibrium for the VDS $\tilde{\Phi}^c(t)$. This is shown as follows.

From the definition of equilibrium point, we have $\nabla \mathcal{I}(\tilde{\Phi}_*; \mathcal{Q}(t)) = \mathbf{0}$ (see equations (15)). Since $\Phi^{[b]}$ and $\Phi^{[l]}$

do not couple in $\mathcal{I}(\tilde{\Phi}; \mathcal{Q})$, we have $\nabla_{\Phi_*^{[b]}} \mathcal{I}(\tilde{\Phi}_*) = \mathbf{0}$, which leads to

$$\mathbf{Q}^{[b]} \Phi_*^{[b]} = \Phi_*^{[b]} \Phi_*^{[b]\dagger} \mathbf{Q}^{[b]} \Phi_*^{[b]}, \quad \forall b$$

due to the gradient equation (14) and the fact that $\Phi^{[b]\dagger} \Phi^{[b]} = \mathbf{I}$ for Algorithm 1. As a result, $\text{span}(\Phi_*^{[b]})$ must span the eigen subspace of $\mathbf{Q}^{[b]}$. That means the columns of $\Phi_*^{[b]} = \Phi_*^{[b]} \mathbf{M}$, where \mathbf{M} is an appropriately chosen unitary matrix, are the eigenvectors of $\mathbf{Q}^{[b]}$.

Using the Lyapunov stability analysis techniques [44], consider a Lyapunov function $V(\tilde{\Phi}^e) = \frac{1}{2} \text{tr} [\tilde{\Phi}^{e\dagger} \tilde{\Phi}^e]$. We write $\tilde{\Phi}^c = (\Phi_c^{[1]}, \dots, \Phi_c^{[b]}, \dots, \Phi_c^{[G]})$ and $\tilde{\Phi}^e = (\Phi_e^{[1]}, \dots, \Phi_e^{[b]}, \dots, \Phi_e^{[G]})$ for each component b , where $\Phi_e^{[b]} = \Phi_c^{[b]} - \Phi_*^{[b]}$. We have

$$\begin{aligned} \dot{V}(\tilde{\Phi}^e) &= \text{tr} \left\{ \text{Re} \left[\tilde{\Phi}^{e\dagger} d\tilde{\Phi}^e \right] \right\} \\ &\stackrel{(a)}{=} -\text{tr} \left\{ \text{Re} \left[\tilde{\Phi}^{e\dagger} F(\tilde{\Phi}^c; \mathcal{Q}(t)) \right] \right\} \\ &\stackrel{(b)}{=} -\sum_{b=1}^G \int_0^1 (1-\mu) \text{tr} \left[\Phi_e^{[b]\dagger} \text{Hess}_{(\Phi_*^{[b]} + \mu \Phi_e^{[b]})}(\Phi_e^{[b]}) \right] d\mu \end{aligned} \quad (26)$$

where equation $\stackrel{(a)}{=}$ is due to $d\tilde{\Phi}_*^c = \mathbf{0}$ under static channels and equation $\stackrel{(b)}{=}$ is obtained from the multi-dimensional Taylor's expansion of $F(\tilde{\Phi}^c; \mathcal{Q}(t))$.

To study the term in $\stackrel{(b)}{=}$, without loss of generality, we consider the columns of $\Phi_*^{[b]}$ are the eigenvectors of $\mathbf{Q}^{[b]}$. From (18), we have

$$\text{Hess}_{\Phi_*^{[b]}}(\Phi_e^{[b]}) = \left(\mathbf{I} - \Phi_*^{[b]} \Phi_*^{[b]\dagger} \right) \left[\mathbf{Q}^{[b]}(\Phi_e^{[b]}) - (\Phi_e^{[b]}) \Psi^{[b]} \right] \quad (27)$$

where $\Psi^{[b]}$ is a diagonal matrix with diagonal elements $\lambda_i^{[b]}$ being the eigenvalues of $\mathbf{Q}^{[b]}$ and $\mathbf{I} - \Phi_*^{[b]} \Phi_*^{[b]\dagger}$ is a projection matrix onto the null space of eigen subspace $\text{span}(\Phi_*^{[b]})$. Therefore, the i -th column of the Hessian (27) is

$$\text{Hess}_{\Phi_*^{[b]}}(\Phi_e^{[b],i}) = \left(\mathbf{I} - \Phi_*^{[b]} \Phi_*^{[b]\dagger} \right) \left(\mathbf{Q}^{[b]} - \lambda_i \mathbf{I} \right) (\Phi_e^{[b],i}) \quad (28)$$

where $\Phi_e^{[b],i}$ denotes the i -th column of $\Phi_e^{[b]}$, and the eigenvalues of the matrix $(\mathbf{I} - \Phi_*^{[b]} \Phi_*^{[b]\dagger}) (\mathbf{Q}^{[b]} - \lambda_i \mathbf{I})$ are either 0 (due to the eigen subspace projection) or $\lambda_j^{[b]} - \lambda_i^{[b]}$, where $\lambda_j^{[b]}$ are the eigenvalues of $\mathbf{Q}^{[b]}$ corresponding to the eigenvectors of the null space of $\Phi_*^{[b]}$.

Therefore, the Lyapunov drift $\dot{V}(\tilde{\Phi}^e)$ in (26) is negative semi-definite if and only if $\lambda_j^{[b]} - \lambda_i^{[b]} \geq 0$ for all j , which means $\Phi_*^{[b]}$ spans the minimum eigen subspace of $\mathbf{Q}^{[b]}$ for each b . In other words, under such choice of $\Phi_*^{[b]}$, the Lyapunov function $V(\tilde{\Phi}^e)$ is always decreasing, unless it reaches the point $\tilde{\Phi}^e = \mathbf{0}$. As a result, Φ_* gives a stable equilibrium.

Note that, due to the distinct eigenvalue condition for $\mathbf{Q}^{[b]}$, the minimum eigen subspace for each $\mathbf{Q}^{[b]}$ is unique. Hence, such stable equilibrium is unique.

As a result, under static channel covariance, the VDS has only one stable equilibrium and it would converge to the unique stable equilibrium w.p.1. This is because when the state trajectory of the VDS passes over the neighborhood of

an unstable equilibrium, there is a high probability for it to be expelled away from the unstable equilibrium and it can only be attracted by the unique stable equilibrium.

B. Proof of Theorem 3

The global attraction property of Algorithm 1 has been established by Lemma 1 using an equivalent continuous-time trajectory. Therefore, Algorithm 1 is guaranteed to converge to the neighborhood of the global unique optimal point $\tilde{\Phi}_*$ even for non-decreasing step size $\gamma > 0$. Moreover, since $\mathcal{I}(\tilde{\Phi})$ is Lipschitz continuous in $\tilde{\Phi}$, using [45, Proposition 3.2.1], for sufficiently small step size $0 < \gamma < \gamma_0$, the gradient algorithm converges to the unique global optimal point under static channels.

APPENDIX D PROOF OF THEOREM 4

Applying Hessian operator at the point $\tilde{\Phi}^c$ to the above compensation algorithm flow (21), we have $\text{Hess}_{\tilde{\Phi}^c}(d\tilde{\Phi}^c) = \text{Hess}_{\tilde{\Phi}^c}(F(\tilde{\Phi}^c; \mathcal{Q}(t))dt + \text{Hess}_{\tilde{\Phi}^c}(\widehat{d\tilde{\Phi}_*})$. From the optimality condition (22), we have

$$\begin{aligned} & \text{Hess}_{\tilde{\Phi}^c}(d\tilde{\Phi}^c) + F(\tilde{\Phi}^c; d\mathcal{Q}) \\ &= \text{Hess}_{\tilde{\Phi}^c}(F(\tilde{\Phi}^c; \mathcal{Q}(t))dt + \text{Hess}_{\tilde{\Phi}^c}(\widehat{d\tilde{\Phi}_*}) + F(\tilde{\Phi}^c; d\mathcal{Q}) \\ &= \text{Hess}_{\tilde{\Phi}^c}(F(\tilde{\Phi}^c; \mathcal{Q}(t))dt. \end{aligned} \quad (29)$$

As an intermediate result, we want to show that the gradient mapping $F(\tilde{\Phi}^c; \mathcal{Q}(t))$ converges to zero, which is a necessary condition for $\tilde{\Phi}^c(t)$ converging to $\tilde{\Phi}_*(t)$. In the following, we construct a Lyapunov function $V(\tilde{\Phi}^c; t) = \frac{1}{2}\text{tr} \left[F(\tilde{\Phi}^c; \mathcal{Q}(t))^\dagger F(\tilde{\Phi}^c; \mathcal{Q}(t)) \right]$ and check the property of the Lyapunov drift \dot{V} .

Using the chain rule gives $dF(\tilde{\Phi}^c(t); \mathcal{Q}(t)) = \text{Hess}_{\tilde{\Phi}^c}(d\tilde{\Phi}^c) + F(\tilde{\Phi}^c; d\mathcal{Q})$, we have

$$\begin{aligned} \dot{V}(\tilde{\Phi}^c; t) &= \text{tr} \left\{ \text{Re} \left[F(\tilde{\Phi}^c; \mathcal{Q}(t))^\dagger dF(\tilde{\Phi}^c(t); \mathcal{Q}(t)) \right] \right\} \\ &= \text{tr} \left\{ \text{Re} \left[F(\tilde{\Phi}^c; \mathcal{Q}(t))^\dagger \left(\text{Hess}_{\tilde{\Phi}^c} \tilde{\Phi}^e + F(\tilde{\Phi}^c; d\mathcal{Q}) \right) \right] \right\} \\ &= \text{tr} \left\{ \text{Re} \left[F(\tilde{\Phi}^c; \mathcal{Q}(t))^\dagger \text{Hess}_{\tilde{\Phi}^c}(F(\tilde{\Phi}^c; \mathcal{Q}(t))) \right] \right\} \end{aligned}$$

where the last equality is from (29).

Note that the function $F(\cdot)$ defined in (15) is a projected gradient of the quadratic function $\mathcal{I}(\cdot)$ defined in (10). Therefore, $F(\cdot)$ is Lipschitz continuous. Thus, when $\tilde{\Phi}^c$ is close enough to $\tilde{\Phi}_*$ (i.e., $\|\tilde{\Phi}^e\|$ is small), $\|F(\tilde{\Phi}^c; \mathcal{Q}(t))\|$ is close to $\|F(\tilde{\Phi}_*; \mathcal{Q}(t))\|$, which equals to 0.

From the analysis of the Hessian (28) in Appendix C, $\eta^\dagger \text{Hess}_{\tilde{\Phi}^{[b]}}(\eta)$ is a negative semi-definite quadratic form, provided that $\lambda_{m+1} - \lambda_m > 0$. Therefore, $\text{tr}\{\text{Re}[F(\tilde{\Phi}^c; \mathcal{Q}(t))^\dagger \text{Hess}_{\tilde{\Phi}^c}(F(\tilde{\Phi}^c; \mathcal{Q}(t)))]\}$ is negative definite as long as $\tilde{\Phi}^c$ is sufficiently close to $\tilde{\Phi}_*$. Mathematically, there exists $\epsilon_1 > 0$, such that for all $\tilde{\Phi}$ in the ϵ_1 -neighborhood of $\tilde{\Phi}_*$, $\tilde{\Phi} \in \mathcal{N}_{\epsilon_1}(\tilde{\Phi}_*(t)) = \{\tilde{\Phi} : \|\tilde{\Phi} - \tilde{\Phi}_*(t)\|_F < \epsilon_1\}$, we have (i) $\dot{V}(\tilde{\Phi}^c; t) < 0$, and (ii) an inverse mapping

$F^{-1} : T_X \text{Grass}(p, N_t) \mapsto \text{Grass}(p, n_t)$ satisfying for all t , under some $k_1 < \infty$,

$$\begin{aligned} \|\tilde{\Phi} - \tilde{\Phi}_*(t)\|_F &= \|F^{-1}(F(\tilde{\Phi})) - F^{-1}(F(\tilde{\Phi}_*(t)))\|_F \\ &\leq k_1 \|F(\tilde{\Phi}) - F(\tilde{\Phi}_*(t))\|_F. \end{aligned}$$

The property $\dot{V} < 0$ implies that $\|F(\tilde{\Phi}^c; \mathcal{Q}(t))\|$ always decreases whenever $\|F\| \neq 0$, from the Lyapunov stability theory [44]. Moreover, since the largest eigenvalue λ_{\max} is bounded, there exists $k_2 < \infty$, such that $\|F(\tilde{\Phi}) - F(\tilde{\Phi}_*(t))\|_F < k_2 \|\tilde{\Phi} - \tilde{\Phi}_*(t)\|_F$ for all t .

As a result, choosing $\delta < \frac{\epsilon_1}{k_1 k_2}$ and $\|\tilde{\Phi}^c(0) - \tilde{\Phi}_*(0)\|_F < \delta$, we must have $\|\tilde{\Phi}^c(t) - \tilde{\Phi}_*(t)\|_F < k_1 k_2 \|\tilde{\Phi}^c(0) - \tilde{\Phi}_*(0)\|_F < k_1 k_2 \delta$ and $\tilde{\Phi}^c(t) \in \mathcal{N}_{\epsilon_1}(\tilde{\Phi}_*(t))$ for all t . Therefore, $\|\tilde{\Phi}^c(t) - \tilde{\Phi}_*(t)\|_F < k_1 \|F(\tilde{\Phi}^c; \mathcal{Q}(t))\|_F \rightarrow 0$.

REFERENCES

- [1] G. Foschini, K. Karakayali, and R. Valenzuela, "Coordinating multiple antenna cellular networks to achieve enormous spectral efficiency," *IEEE Proceedings on Communications*, vol. 153, no. 4, pp. 548–555, 2006.
- [2] H. Dahrouj and W. Yu, "Coordinated beamforming for the multicell multi-antenna wireless system," *IEEE Transactions on Wireless Communications*, vol. 9, no. 5, pp. 1748–1759, 2010.
- [3] Q. Shi, M. Razaviyayn, Z.-Q. Luo, and C. He, "An iteratively weighted MMSE approach to distributed sum-utility maximization for a MIMO interfering broadcast channel," *IEEE Transactions on Signal Processing*, vol. 59, no. 9, pp. 4331–4340, 2011.
- [4] B. Zhuang, R. A. Berry, and M. L. Honig, "Interference alignment in MIMO cellular networks," in *IEEE International Conference on Acoustics, Speech and Signal Processing (ICASSP)*. IEEE, 2011, pp. 3356–3359.
- [5] M. Guillaud and D. Gesbert, "Interference alignment in partially connected interfering multiple-access and broadcast channels," in *IEEE Global Telecommunications Conference (GLOBECOM 2011)*. IEEE, 2011, pp. 1–5.
- [6] S. Sanayei and A. Nosratinia, "Antenna selection in MIMO systems," *IEEE Communications Magazine*, vol. 42, no. 10, pp. 68–73, 2004.
- [7] I. Berenguer, X. Wang, and V. Krishnamurthy, "Adaptive MIMO antenna selection via discrete stochastic optimization," *IEEE Transactions on Signal Processing*, vol. 53, no. 11, pp. 4315–4329, 2005.
- [8] A. Adhikary, J. Nam, J. Ahn, and G. Caire, "Joint spatial division and multiplexing—the large-scale array regime," *IEEE Transactions on Information Theory*, vol. 59, no. 10, pp. 6441–6463, Oct 2013.
- [9] A. Adhikary and G. Caire, "Joint spatial division and multiplexing: Opportunistic beamforming and user grouping," *arXiv preprint arXiv:1305.7252*, 2013.
- [10] P. Comon and G. H. Golub, "Tracking a few extreme singular values and vectors in signal processing," *Proceedings of the IEEE*, vol. 78, no. 8, pp. 1327–1343, 1990.
- [11] B. Yang, "Projection approximation subspace tracking," *IEEE Transactions on Signal Processing*, vol. 43, no. 1, pp. 95–107, 1995.
- [12] W. Utschick, "Tracking of signal subspace projectors," *IEEE Transactions on Signal Processing*, vol. 50, no. 4, pp. 769–778, 2002.
- [13] A. S. Poon, D. N. TSe, and R. W. Brodersen, "An adaptive multiantenna transceiver for slowly flat fading channels," *IEEE Transactions on Communications*, vol. 51, no. 11, pp. 1820–1827, 2003.
- [14] Y. Hua, Y. Xiang, T. Chen, K. Abed-Meraim, and Y. Miao, "Natural power method for fast subspace tracking," in *Neural Networks for Signal Processing IX (IEEE Signal Processing Society Workshop 1999)*. IEEE, 1999, pp. 176–185.
- [15] G. Xu and T. Kailath, "Fast subspace decomposition," *IEEE Transactions on Signal Processing*, vol. 42, no. 3, pp. 539–551, 1994.
- [16] J. Tong, P. J. Schreier, and S. R. Weller, "Design and analysis of large MIMO systems with Krylov subspace receivers," *IEEE Transactions on Signal Processing*, vol. 60, no. 5, pp. 2482–2493, 2012.
- [17] B. Niu and A. M. Haimovich, "Interference subspace tracking for network interference alignment in cellular systems," in *Global Telecommunications Conference, 2009. GLOBECOM 2009. IEEE*. IEEE, 2009, pp. 1–5.
- [18] L. M. Correia, *Wireless flexible personalized communications*. John Wiley & Sons, Inc., 2001.

- [19] A. Abdi and M. Kaveh, "A space-time correlation model for multielement antenna systems in mobile fading channels," *IEEE Journal on Selected Areas in Communications*, vol. 20, no. 3, pp. 550–560, 2002.
- [20] M. Zhang, P. J. Smith, and M. Shafi, "An extended one-ring MIMO channel model," *IEEE Transactions on Wireless Communications*, vol. 6, no. 8, pp. 2759–2764, 2007.
- [21] A. Abdi, J. A. Barger, and M. Kaveh, "A parametric model for the distribution of the angle of arrival and the associated correlation function and power spectrum at the mobile station," *IEEE Transactions on Vehicular Technology*, vol. 51, no. 3, pp. 425–434, 2002.
- [22] A. Forenza, D. J. Love, and R. W. Heath, "Simplified spatial correlation models for clustered MIMO channels with different array configurations," *IEEE Transactions on Vehicular Technology*, vol. 56, no. 4, pp. 1924–1934, 2007.
- [23] T. Yoo and A. Goldsmith, "On the optimality of multiantenna broadcast scheduling using zero-forcing beamforming," *IEEE Journal on Selected Areas in Communications*, vol. 24, no. 3, pp. 528–541, 2006.
- [24] H. Kim, H. Yu, Y. Sung, and Y. H. Lee, "An efficient algorithm for zero-forcing coordinated beamforming," *IEEE Communications Letters*, vol. 16, no. 7, pp. 994–997, 2012.
- [25] K. Gomadam, V. R. Cadambe, and S. A. Jafar, "Approaching the capacity of wireless networks through distributed interference alignment," in *IEEE Global Telecommunications Conference (GLOBECOM 2008)*, IEEE, 2008, pp. 1–6.
- [26] T. L. Marzetta, "Noncooperative cellular wireless with unlimited numbers of base station antennas," *IEEE Transactions on Wireless Communications*, vol. 9, no. 11, pp. 3590–3600, 2010.
- [27] X. Zhang, A. F. Molisch, and S.-Y. Kung, "Variable-phase-shift-based RF-baseband codesign for MIMO antenna selection," *IEEE Transactions on Signal Processing*, vol. 53, no. 11, pp. 4091–4103, 2005.
- [28] P. Sudarshan, N. B. Mehta, A. F. Molisch, and J. Zhang, "Channel statistics-based RF pre-processing with antenna selection," *IEEE Transactions on Wireless Communications*, vol. 5, no. 12, pp. 3501–3511, 2006.
- [29] C. Suh and D. Tse, "Interference alignment for cellular networks," in *The 46th Annual Allerton Conference on Communication, Control, and Computing*. IEEE, 2008, pp. 1037–1044.
- [30] J. H. Manton, "Optimization algorithms exploiting unitary constraints," *IEEE Transactions on Signal Processing*, vol. 50, no. 3, pp. 635–650, 2002.
- [31] P.-A. Absil, R. Mahony, and R. Sepulchre, *Optimization algorithms on matrix manifolds*. Princeton University Press, 2009.
- [32] L. W. Tu, *An introduction to manifolds*. Springer, 2011.
- [33] D. Bertsekas, "Nonlinear programming," 1999.
- [34] S. Boyd and L. Vandenberghe, *Convex Optimization*. Cambridge University Press, 2004.
- [35] E. Lundström and L. Eldén, "Adaptive eigenvalue computations using Newton's method on the Grassmann manifold," *SIAM journal on matrix analysis and applications*, vol. 23, no. 3, pp. 819–839, 2002.
- [36] G. H. Golub and C. F. Van Loan, *Matrix computations*. JHU Press, 2012, vol. 3.
- [37] J. Chen and V. Lau, "Convergence analysis of saddle point problems in time varying wireless systems - control theoretical approach," *IEEE Transactions on Signal Processing*, vol. 60, no. 1, pp. 443–452, January 2012.
- [38] J. Chen and V. K. N. Lau, "Convergence analysis of mixed timescales cross-layer stochastic optimization," *submitted to IEEE Transactions on Information Theory*, April 2013. [Online]. Available: <http://arxiv.org/abs/1305.0153>
- [39] "Technical specification group radio access network; evolved universal terrestrial radio access (e-utra); further advancements for e-utra physical layer aspects," 3GPP TR 36.814, Tech. Rep., 2010. [Online]. Available: <http://www.3gpp.org>
- [40] K. Baddour and N. Beaulieu, "Autoregressive models for fading channel simulation," in *Global Telecommunications Conference, 2001. IEEE GLOBECOM '01.*, vol. 2, 2001, pp. 1187–1192 vol.2.
- [41] H. M. Moller, "Exact computation of the generalized inverse and the least-squares solution," Universitat Dortmund, Germany, Tech. Rep., 1998.
- [42] S. H. Chae and S.-Y. Chung, "On the degrees of freedom of rank deficient interference channels," in *IEEE International Symposium on Information Theory Proceedings (ISIT)*, 2011, pp. 1367–1371.
- [43] H. Kushner and G. Yin, *Stochastic approximation and recursive algorithms and applications*. Springer, 2003, vol. 35.
- [44] H. K. Khalil, *Nonlinear Systems*. Prentice-Hall, 1996.
- [45] D. P. Bertsekas and J. N. Tsitsiklis, *Parallel and distributed computation*. Old Tappan, NJ, USA: Prentice Hall Inc., 1989.



Junting Chen (S'11) received the B.Sc. degree in electronic science and technology from Nanjing University, Nanjing, China, in 2009. He is with the Department of Electronic and Computer Engineering, The Hong Kong University of Science and Technology (HKUST), Hong Kong, where he is now a Ph.D. candidate.

Since February 2014, he has been in the Laboratory for Information and Decision Systems (LIDS) at Massachusetts Institute of Technology (MIT) as a visiting student. His research interests include beamformer design in massive MIMO systems, resource allocations and cross-layer optimizations in wireless communication networks, and algorithm design and analysis under time-varying channels.



Vincent K. N. Lau (SM'04) received the B.Eng. (Distinction 1st Hons.) from the University of Hong Kong in 1992 and the Ph.D. degree from Cambridge University, Cambridge, U.K., in 1997.

He was with HK Telecom (PCCW) as a System Engineer from 1992 to 1995, and with Bell Labs - Lucent Technologies as a member of Technical Staff during 1997-2003. He then joined the Department of ECE, HKUST, and is currently a Professor. His current research interests include the robust and delay-sensitive cross-layer scheduling of MIMO/OFDM wireless systems, cooperative and cognitive communications, dynamic spectrum access, as well as stochastic approximation and Markov decision process.